INVESTIGATION OF GROUND VIBRATIONS DUE TO MOVING TRAINS

Phapetha Thadsanamoorthy

208041R

Degree of Master of Science

Department of Civil Engineering

University of Moratuwa

Sri Lanka

July 2023

INVESTIGATION OF GROUND VIBRATIONS DUE TO MOVING TRAINS

Phapetha Thadsanamoorthy

208041R

Thesis submitted in partial fulfilment of the requirements for the degree Master of Science in Civil Engineering

Department of Civil Engineering

University of Moratuwa

Sri Lanka

July 2023

DECLARATION OF THE CANDIDATE & SUPERVISOR

I declare that this is my own work and this thesis does not incorporate without acknowledgement any material previously submitted for a for a Degree or Diploma in any other University or institute of higher learning and to the best of my knowledge and belief it does not contain any material previously published or written by another person except where the acknowledgement is made in the text.

Also, I hereby grant to University of Moratuwa the non-exclusive right to reproduce and distribute my thesis, in whole or in part in print, electronic or other medium. I retain the right to use this content in whole or part in future works (such as articles or books).

Signature: Date: 09/07/2023

The above candidate has carried out research for the Masters under my supervision

Name of the supervisor: Dr. H. G. H. Damruwan

Signature of the supervisor: Date: 10/07/2023

Name of the supervisor: Prof. C. S. Lewangamage

Signature of the supervisor: Date: 10/07/2023

ABSTRACT

This research focuses on the assessment of train-induced ground vibrations through experimental analysis and the development of a Finite Element (FE) prediction model. The study aims to evaluate the intensity of vibrations caused by trains and understand their effects on different soil types and train speeds.

A vibration sensing device named "VIBSEN" was developed for the measurement of ground vibrations. Experimental data were collected at 3m intervals from the centreline of the railway track and processed using MATLAB software. The accuracy of the device was confirmed through gravity calibration and comparison with a vibrometer. Based on the experimental study conducted at a specific site, it was determined that the minimum safe distance from the centreline of the track is approximately 10m when two trains cross simultaneously and approximately 6m when considering the passage of a single train. It should be noted that these recommendations are specific to the soil profile at the experimental site and may vary depending on subgrade soil type and parameters.

The FE prediction model, developed using MIDAS GTS NX FE software, was validated using experimental results from the study and further compared with literature data. The model successfully predicted train-induced ground vibrations, demonstrating its applicability. Parametric analysis was conducted to investigate the effects of soil type and train speed on vibration intensity, including the identification of resonance frequencies and critical velocities. The findings of the study indicate that vibration intensity varies significantly depending on the soil type, with lower intensities observed for soils with higher elastic moduli. Additionally, the study highlighted that vibration intensity increases with train speed, and certain speed levels may lead to a sudden increase in intensity due to resonance effects. The resonance frequency was found to be influenced by the elastic modulus of the subgrade soil.

Overall, this study provides valuable insights into train-induced ground vibrations and offers recommendations for safe distances from the track centreline. The developed VIBSEN device and FE prediction model offers reliable tools for future investigations and allow for parametric studies considering different soil properties, train loads, and speeds. These findings contribute to mitigating risks, minimizing structural failures, and reducing hazards associated with prolonged exposure to vibrations.

Keywords: Train-induced ground vibration; VIBSEN device; Peak Particle Velocity (PPV); Finite Element (FE) prediction model.

ACKNOWLEDGEMENT

I wish to acknowledge the financial support provided by the Senate Research Committee (Grant - SRC/LT/2020/17), University of Moratuwa, Sri Lanka to undertake this research. In addition to that, I take this opportunity to express my sincere gratitude to the individuals who have guided me and supported throughout the entire journey to successfully finish this research study.

I would like to extend my heartiest gratitude to my supervisors Dr. H. G. H. Damruwan, Senior lecturer, Department of Civil Engineering, University of Moratuwa, and Prof. C. S. Lewangamage, Professor, Department of Civil Engineering, University of Moratuwa, for the immense trust, support and guidance provided throughout the entire duration to successfully complete this research.

My special thanks to Prof. M. T. R. Jayasinghe and Prof. J. C. P. H. Gamage for the valuable advice and comments given in the progress presentations. My sincere thanks to Prof. (Mrs). C. Jayasinghe, Head, Department of Civil Engineering, University of Moratuwa, for her immense support in providing necessary facilities and provisions in completing this study. I am indebted to give my gratitude to Eng.K.Pirunthan for his immense support in enhancing my understanding and knowledge in electronic device development.

Furthermore, my sincere gratitude to the staff of Department of Railways, Sri Lanka, the academic and non-academic staff of the Department of Civil Engineering, University of Moratuwa for their guidance and support to complete this research study. I'm grateful for all the previous researchers for undertaking successful research and making them available for the upcoming researchers. Last but not least, I am extending my humble gratitude for all my friends and colleagues for supporting me in all the ways they could.

Phapetha Thadsanamoorthy,
Department of civil engineering,
University of Moratuwa

TABLE OF CONTENTS

LIST OF FIGURES

LIST OF TABLES

LIST OF ABBREVIATIONS

FE – Finite Element

FEM – Finite Element Model

SHM – Structural Health Monitoring

HST – High-speed train

LRT – Light rail transit

PPV – Peak Particle Velocity

TGV – Train à Grande Vitesse

LIST OF APPENDICES

1. INTRODUCTION

1.1 Background

Ground vibrations are generated due to human activities of varying severity, ranging from high intense activities such as explosion, blasting, and heavy vehicular movement to insignificant activities such as jumping, digging, and even walking on the ground. The intensity of generated ground borne vibration is dependent on the magnitude of the source activity and the characteristics of receiving body. There is no any particular methodology to categorize the severity of the vibration since the human perception and sensitivity is one of the key components of classification. The person who is highly sensitive to the noise feels discomfort in even minor level of vibration. Although there are various sources of vibration generation, this study is focused on the investigation on the effects of ground vibration generated due to the train movements.

Railway service is one of the most effective mass modes of transport which helps in the passage of both people and goods. It is economical, efficient, comfortable, and eco-friendly. Unlike the other modes of transport, train passage is climate-safe, independent on fog, mist, or rain. It is believed that the invention of rail transport is one of the quintessential factors in industrial revolution of Western Europe. Since then, the developed and developing countries concentrate more on developing rail infrastructure in terms of speed, comfort, capacity, and travel distance to plan for the future. Nowadays, a variety of train types are available to satisfy wide range of user requirements. High-speed trains, light rails, monorails, and commuter rails are few of most.

In Sri Lanka, the railway services have a great history since 19th century initiated to transport coffee from the hills of Kandy to Colombo-Fort on its way to European market. Later, coastal railway lines along West and South-West were initiated to accumulate coconut from the coastal belt, and Eastern railway lines were built focusing on Trincomalee harbour and the provincial capital Batticaloa. A new track line was laid from Kankesanthurai to Colombo-fort via Annuradhapura to transport

cheap labour from India to the plantations. Hence, these railway networks still prevail and in use, commuting thousands of people as a run-of-the-mill. Sri Lanka is one of the countries, who is set far back in advanced rail technology. The prior statement is indorsed by still using the first laid rail tracks and time-worn trains serving the present demand.

Like the other sources of vibration, train induced vibration is generated when the wheel force is transferred to the rails followed by sleepers through elastic rail pads. The sleepers dissipate the energy to ballast and sub-ballast layers and transfers to the subgrade. The waves penetrate through the medium and propagates in all directions dominating outwards the track, till the energy approaches to null. Wave pattern of vibration propagation is not unique. There are 3 major wave types influences in train induced energy transfer.

1. Surface waves (Reileigh wave) – reduces with distance. Inversely proportional to square root of distance, Slower than P and S waves
2. Compression waves (P-waves) – Faster than other two waves
3. Shear waves (S-waves) – Faster than surface waves but slower than P waves

Surface waves are the dominant waves in ground borne wave propagation. According to the previous research, 67% of total energy is dissipated as surface waves (Miller et al., 1955). The intensity of vibration is inversely proportional to the propagating distance as the wave energy dissipates during the passage in various forms. Several factors affect the train induced ground borne vibration as indicated below.

1. Type of train
2. Speed
3. Load
4. Ground properties
5. Wheel-rail-track irregularities

Influence of train type on vibration is essential as it includes the train load, fuel used, speed and train component system. The Table 1-1 below shows the effects of train

type on train induced ground vibration (Al Suhairy & Chalmers University of Technology. The Department of Technical Acoustics., 2000).

Table 1-1: Influence of train type in vibration

Train type	**Problem**
Steel wheel urban rail transit	Noise and vibration are common within 150m range. The intensity of the inconvenience due to vibration depends on the geology of the location and the building structure.
Commuter and intercity passenger trains	Most commonly the track is shared with the freight trains which has a different vibration level.
High speed passenger trains	Wheel flats which can create higher induced vibration are more common
Automated guideway transit system	Ground-borne vibration problems are rare because of the low speed and lightweight

Source: Al Suhairy, (2000)

Even though, we could measure the vibration intensity using digital and analog devices, human perception, and sensitivity influences in deciding the level of disturbance. However, various standards have been established to distinguish the tolerable limits of vibration intensity for various purposes. DIN 4150-3 defines the building vibration as a mechanical oscillation having ability to damage the structure or cause discomfort to occupants. This standard also known as German standard, which categorizes the vibration effects into four cases: a) damage to building, b) damage to building contents, c) disturbance to human comfort, and d) audible effects. This also provides complete details on how to measure the vibration. IEST standard guides to use RMS vibration velocity in one third octave band to measure the vibration. Apart from these, the vibration standards ISO 10816-2 (2009), ISO 2631-

1(1997), DIN 4150-2(Jun1999), BS 7385-2(1993) and BS6472-1(2008) also discuss about the vibration on machines, buildings and ground.

According to Svinkin & Asce, (2014) the vibration triggers oscillation at many locations of the building. This is addressed as the direct vibration effect which could lead to cracking of structural components. This is observed as a serious issue in old buildings being exposed to persistent vibration. Also, the vibration directly affects the structure by relocating the soil particles of ground either by loosening or compacting. Prolonged displacement for a long period of time can collapse the building like a house of cards collapsing completely after the removal of single card in the stack. Apart from the building damages, occupants may also feel discomfort due to noise and vibration reception. The research study of Vithrana et al., (2013) states that this may also lead to serious health hazards and long term impacts on human health. Zhu et al., (2014) imposes the necessity to account for the influence of construction vibration on the precision of medical equipment in his research work which compares the level of allowable vibration and predicted vibration levels and elaborates the level of potential risk to the functionality of the devices.

This study was focused on measuring on site ground borne vibration induced due to train movements and analysing their behaviour depending on the influential parameters. Furthermore, a three-dimensional (3D) Finite Element (FE) model was developed to predict the intensity of ground borne vibration. A parametric study was carried out to explore the effects of parameters such as train speed, distance form the railway track and soil type on the train induced ground vibration.

1.2 Problem statement

Even though Sri Lanka is having long spanning history in railway services, it is one of the most underdeveloped local services compared to the neighbouring countries. The phrase underdeveloped includes the poor infrastructure development, lack of exposure to latest technologies and poor investment in research study. It requires proper analysis of the effect of existing structure as well as proposed modifications before implementing a change for effective results. Furthermore, regular monitoring

will pay way to reduce the loss to life and property before severe disaster. Exclusively vibration analysis induced due to train movements is utmost essential for the better performance of railway services.

Experimental investigation is the conventional method of vibration analysis. It involves the use of vibration sensing devices to measure the intensity of vibration. The accuracy of the results varies based on the sensitivity of the sensing and recording devices. Better experimental results provide a way for efficient analysis. Despite of the advantages, this is expensive, time consuming and difficult to derive all the parameters influencing the environment of the experiment. From train to train and location to location the parameters may vary drastically, and it is hard to find two scenarios with identical parameters. Hence, that makes it hard to predict the intensity of vibration from only one experimental result. In countries like Sri Lanka, the availability of equipment and devices to monitor the vibration is countable. Furthermore, analysing the behaviour at a location requires numerous data points collected over the repeating experiments for several different changing parameters (Degrande & Schillemans, 2001). This part of the study requires more time duration as well as human resources.

On the other hand, researchers have developed FE models using computer software to predict the ground vibration due to moving trains by adapting to various theories. It is evident that a proper FE model will reduce the cost and time for the vibration analysis while maintaining the accuracy to the desired level. This research is based on developing a user-friendly 3D FE model using MIDAS GTS NX software to slash the shortcomings of the conventional vibration monitoring system.

1.3 Aim and objectives.

The aim of this research is to investigate the ground vibration caused by train movements and analyse the impact of various influencing parameters, including train speed, distance from the railway track, and soil type, on the train-induced ground vibration. The aim of this study is achieved by accomplishing the following objectives:

- Develop a sensor-based portable electronic device capable of monitoring vibration intensity in all three directions.
- Conduct on-site experimental analysis using the developed device to assess the vibrations induced by local trains.
- Develop a FE Prediction Model using the MIDAS GTS NX software to investigate the train induced ground vibration and validate it using the results obtained from the experiments.
- Perform a parametric study using the developed FE model to investigate the effects of various factors such as train speed, distance from the railway track, and soil type on the train-induced ground vibration.

1.4 Significance of the Research

The vibrations caused by train movements are considered a significant problem for both passengers and residents in the vicinity. Traditional experimental analysis methods are costly, time-consuming, and require a large amount of manpower to assess induced vibrations and their effects. As a result, on-site testing is often lacking. This research aims to develop a numerical prediction model that can reliably and accurately predict train-induced vibrations while minimizing costs, time, and resources. The model is designed to be versatile, capable of producing accurate results for various scenarios involving different soil types, train loads, and other material and non-material properties. This prediction model is highly valuable to the Department of Railways, enabling them to predict vibration intensity, test for subgrade deformation, monitor the train-track-ground system for maintenance and mitigation purposes, as well as assisting other sectors in assessing, monitoring, and mitigating vibrations and their effects.

1.5 Arrangement of the Thesis

Chapter 1 provides a concise introduction to the research project, outlining the research problem, aim and objectives, as well as highlighting the significance of the study. It sets the foundation for the subsequent chapters by giving an overview of the

project. The outline of each chapter is also provided, giving a glimpse of the overall structure and content of the thesis.

Chapter 2 gives the literature review of past research work undertaken on this subject area under different categories such as the way of train-induced ground vibration generation and propagation, factors influencing the intensity of vibration, the international guidelines on vibration, methods of monitoring and analysis, experimental analysis of ground vibration, FE modelling, ground properties and track properties, theories followed in FE modelling of the track elements, effects of vibration on human and structures and the ways of mitigation. This will give a brief idea about the research gap and identification of the new areas.

Chapter 3 serves as an in-depth exploration of the methodology followed in this study, which is organized into three main sections: gadget development and field experimental analysis, development of the FE prediction model and validation, and parametric analysis using the FE prediction model. This chapter provides comprehensive knowledge about each activity performed within every section. It includes the components and functions of the gadget, the identification of experimental locations, the process of data collection and processing, the utilization of MIDAS GTS NX software for FE modelling, the identification of component functions and modelling based on respective theories, signal processing of field data using MATLAB, the validation of the model by referencing a previous experimental study, ensuring results by comparing the FE results with the present field analysis results, and conducting parametric analysis using the FE prediction model to address the effects of influencing factors

Chapter 4 presents the results and discussion of the investigations conducted as elaborated in chapter 3. The field experimental results and the FE simulation results have been presented graphically for easy visualization and understanding. The experimental data includes measurements of vibration intensity and attenuation along with the corresponding distances. The FE simulation results illustrate the vibration intensity in terms of Peak Particle Velocity (PPV) at selected distances, examining the impact of speed, subgrade strength, and critical velocity.

Chapter 5 presents the conclusions and recommendations of this study based on the obtained results. The specific topic of this research holds a broad scope and offers potential for further enhancement in numerous ways. This chapter provides comprehensive insights into areas that should be prioritized for future research, both at the national and international levels.

2. LITERATURE REVIEW

2.1 Introduction

A moving body generates moving stress pattern around and beneath to maintain stability according to the law of motion. Stress waves propagate through various mediums to dissipate occupied energy in multiple modes. In general, body waves and surface waves are the two categories of propagating waves. Among the body waves, compression waves and shear waves propagate through the soil and rock medium. The Rayleigh wave of surface wave type are the dominant waves who occupies two third of the total energy generated by the train induced vibration (Al Suhairy & Chalmers University of Technology. The Department of Technical Acoustics., 2000). The direction of particle motion for each wave is different and it is described below.

- Compression waves: oscillation takes place in a motion along the direction of propagation.
- Shear waves: oscillation takes place on a plane normal to the direction of propagation.
- Rayleigh waves: Particle motion take place in elliptical path in a vertical plane through the direction of propagation.

Ideally, in a homogenous ground condition, compression waves and the shear waves propagate in all direction away from the source, therefore substantial geometric attenuation and damping takes place. But the Rayleigh waves do not suffer geometric attenuation but loses energy due to damping. However, in practical the ground is far away from homogeneity therefore mode conversions from one type to the other takes place. Each vibration mode has unique velocity and vibration energy depending on soil parameters. Further, the waves with higher frequencies attenuate more rapidly than the waves with lower frequencies. This makes lower frequency waves more critical.

Throughout the entire research history, train induced vibration analysis has drawn the interest of many researchers around the world. Since the 19^{th} century, extensive research has been conducted on various aspects related to train-induced vibration.

This includes studies on the generation of vibrations, different types of ground conditions, components of rail infrastructure, materials used in construction, the influence of various factors on vibration intensity and propagation, and the effects of vibration on both living and non-living entities. Both conventional and computer simulation techniques have been employed in this research to study railway-induced ground-borne vibrations. The purpose of this literature review is to identify the contributions of past researchers in the field of railway-induced ground-borne vibration and its related areas. This review aims to explore topics such as ground-borne vibration, methods of analysis for railway-induced vibration, parameters that influence vibration intensity, and the effects of vibrations on buildings, occupants, and users. By examining the existing body of knowledge, this review seeks to provide a comprehensive understanding of the research conducted in this domain.

2.2 Influence of ground profile in the intensity of train induced vibration

Ground type is one of the key components affecting vibration intensity. The engineers lay the rail tracks along varying natural ground conditions such as embankment, flat land, at-grade, low land, and man-made structures such as tunnels and bridges. Together with this, the type of soil will also influence on the vibration intensity. Hence study on the effects of railway vibration on various soil profiles and ground conditions is being encouraged. More importance is given to study the effects of High-speed trains (HST) HST rather than Light rail transit (LRT) due to the drastic variance in speed parameter. Despite of this, LRT should also be studied carefully due to the other possibilities such as denser building construction which pioneer in causing adverse effects.

Madshus & Kaynia,(2000) used experimented on the negative effects of vibration on soft soil ground and developed numerical analysis to second the findings. Authors concluded that, magnificent increase in vibration level at critical speed can create numerous hazardous effects such as train derailment, operational issues, track degradation etc. Xu et al.,(2017) were interested on the behaviour of rock slopes when exposed to train vibration which paved way for their study. They used wireless

system to monitor the intensity and record. Their research findings include two things: a) the vibration is high near the track and gradually reduced with increasing distance, b) the PPV at 12m distance is 0.4 mm/s which is below the safe limit.

D. P. Connolly et al.,(2014) carried out an experiment on ground borne vibration on four different earth profiles such as at-grade, embankment, cutting and overpass and presented the results. This is considered as one of the excellent works which allows the scholars to compare the effects derived from four different ground conditions.

The vibration levels are measured in three directions up to 100m from the track for three different types of trains namely Eurostar, TGV and Thalys. As a contrary to the common theory, they found that the horizontal vibration also dominates sometimes, more importantly at large offsets. This has paved way to think about the horizontal vibration as equally important as other directions. The result of the study is produced in Figure 2.1.

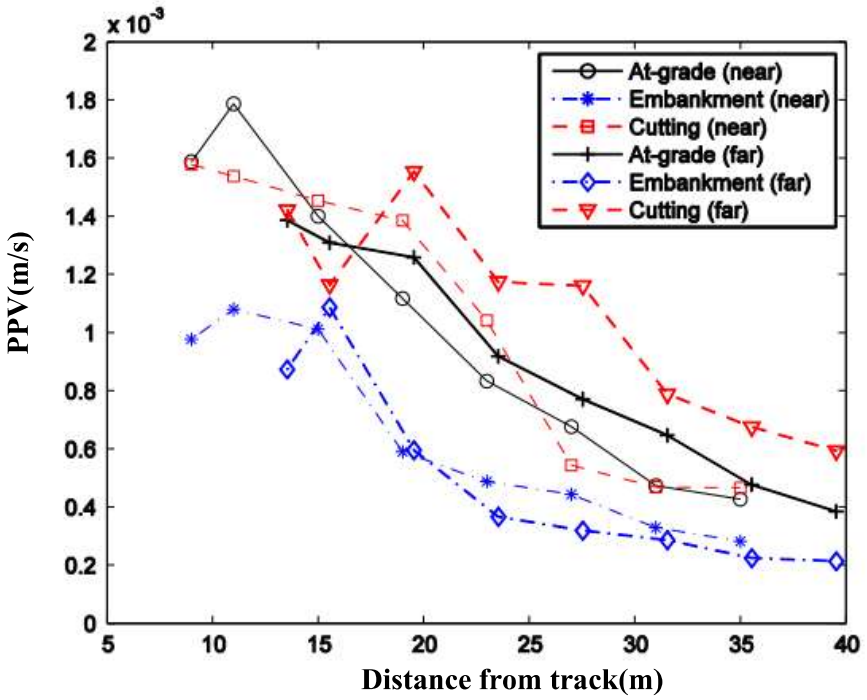

Figure 2.1: Vertical vibration levels generated due to near and far train passages

2.3 Approaches of Vibration Analysis

2.3.1 Experimental analysis

Physical experiments were the primary way of vibration assessment in early times adopted by many researchers. The standard procedure to be followed when undertaking the experiment, the general guidance on the train induced ground borne noise and vibration (ISO 14837-1, 2005), the operation of the rail system and the resultant noise effects in the adjoining buildings (BS 7385-1, 1990)(BS 7385-2, 1993), evaluation of mechanical vibration (BS ISO 10816-7, 2009) and evaluation of human exposure to whole body vibration(ISO 2631-1, 1997) are standardized in order to ensure the international standard and uniformity. The parameters and factors that should be taken into consideration is listed together with the guidance on prediction models. The field measurement guideline recommends measuring the vibration intensity in a line perpendicular to the track in three dimensions, to quantify the intensity of vibration amplitude.

Among the conventional experimental researchers, Correia et al., (2016), did the experiment along a stretch of Portuguese railway network by analysing the induced vibration effect of 20 trains. The variability of the result is discussed and made the raw data accessible for the researchers. Similarly experiment along the high-speed rail lines between Brussels and Koln by Lombaert et al., (2006), investigation on ground vibration induced by subway vehicles and radiated noise on buildings in China by Li et al., (2016), study on attenuation of vibration induced by heavy freight wagons in China by Hu et al., (2018) and experiment of Georges Kouroussis et al., (2013) along the high speed rail network are few of the pioneer works done so far.

The experimental analysis of Thalys High Speed train at varying speed done by Degrande & Schillemans,(2001) is one of the major cited work in this genre. Free field vibration and track responses were measured for Thalys HST moving with varying speed between 223 km/h and 314 km/h (61.9 - 87.2 m/s) and analysed about the influence of train speed in recorded parameters. The experimental data set was provided open for researchers for future work.

Deraemaeker et al. (2008) encounters the problem of damage detection using output only method under varying environmental conditions. Eigen vectors and Fourier transform of signals have been used for analysis. The sensitivity of the damage detection procedure to various features have been studied and estimated time to extract different features is summarized.

Lopes et al.,(2016) carried out experimental investigations regarding the assessment of vibration inside buildings due to subway train traffic, to validate a prediction model already proposed by the authors. The numerical model consists of three autonomous models to stimulate vibration generation, propagation, and reception. The scope of the study is attained by taking a comparison between the results from numerical analysis and experiment and ensuring a good agreement among them.

The irregularities in the wheel-track interface and certain shapes of track components and materials also influence vibration. Conventionally, the rectangular shaped sleepers are being used globally for track system. Bogacz, (2015) considered the influence of the component shape and investigated about the effects of two types of sleepers in vibration generation. The findings claim that the Y type sleepers have low amplitude, and low acoustic emission together with low wear. When considering about the properties of materials, cyclic loading of trains degrades the strength. Indraratna & Nimbalkar, (2013) carried out the cyclic drained test on a segment of model rail track on a geosynthetically reinforced railroad ballast track. The findings say that the capacity of the track was enhanced by both the type of reinforcement and its layout.

Apart from ground-based field measurements, vibration induced in man-made structures are also tested. A dynamic monitoring system was installed at concrete arch bridge at city of Porto by Magalhaes et al.,(2012) to create a complete database of structure response to ambient excitation. Yang et al.,(2018) carried out experimental analysis to identify the effects of ground borne vibration from shield tunnels. He developed three physical tunnel lining models and the response behaviour of all three models were compared.

The code of practice recommends the vibration intensity to be equal to or less than the recommended value. However, it is not always possible to have less intense vibration. Therefore, mitigation measures can be suggested to reduce the level of vibration to the desired level. Several mitigation methods have been tested since long time. Jayawardana et al., (2018) identified the use of trenches in reducing the vibration by using experimental and numerical analysis for Sri Lankan context.

2.3.2 The numerical FE prediction model

In order to overcome the high cost and time consumption for the experimental study, Lombaert et al.,(2006) suggested to develop a numerical prediction model based on the actual data. His research work presents experimental validation for the numerical track-soil model assuming the track section and properties are invariant along the track. The numerical system is modelled as a longitudinally invariant system located on a horizontally layered elastic half space. Field experiments were done on HST L2 line between Brussels and Koln. Soil and track properties were measured in the initial stage of experiments. Dynamic soil properties have been found from the Seismic cone penetration test (SCPT) and spectral analysis of surface waves (SASW). Rail receptance test was done to find the track parameters. In the later stage, the free field – steel foundation transfer functions and the track-free field transfer functions were used to validate the numerical model. Given the large number of modelling uncertainties, the numerical results show good agreement with the experimental results ensuring the suitability to use it for future predictions.

Modelling of track-soil components play a crucial role in the precision of numerical results and simulation duration. Finer meshes will give higher accuracy but takes a long processing time. Selection of optimum mesh size is essential. The mesh size will directly influence the number of nodes per element, and it is proportional to the number of equations to be solved. Nasasira Derrick, (2020) analysed about the interaction of soil and reinforced cement concrete raft foundation on sandy soil using both analytical and FE analysis. His one of the main findings seconds the statement “finer mesh will produce more accurate results compared to others”.

When modelling the rail and concrete sleepers, they could be considered as elastic materials and other components are considered as elasto-plastic using Mohr-Coulomb law(Press, 2015). Lombaert et al., (2006) modelled rail as Euler-Bernoulli beam considering the relatively small frequency from 0-400 Hz with bending stiffness and mass. According to Krylov,(1994) the sleepers can be considered as point-source vertical load. Rail pads can be considered as continuous spring damper connections and sleepers are considered not to impact on longitudinal stiffness allowing to model as uniform load. Madshus & Kaynia, (2000) modelled track as a beam element. The track impedance and soil impedance were calculated based on disc Green's function for a horizontally layered half space. Georges Kouroussis et al., (2011) modelled the vertical boundaries as viscous boundary to absorb incident S and P waves.

Conventionally, the track was considered as a beam a continuous support (subgrade or foundation) and could be categorized as one-dimensional problem for simple analysis. Concept of Beam on Elastic foundation, Wrinkler's theory and Zimmermann method could be used to simply solve it. However, for complex analysis such as Finite element analysis (FEA) and Finite element method (FEM) more advanced methods are required. Prakoso,(2012) in his research has combined both conventional and advanced methods by modelling the track system using FEM to model in 2D and 3D and the results are verified using conventional Zimmermann method. Higher accuracy between both methods is observed in 2D model and slight deviation was observed in 3D possibly due to the variation of support condition and contact elements. M. A. Sayeed & Shahin, (2016) modelled rail as 1D I beam section with UIC 60 properties whereas all the other elements were modelled as 3D solids.

Press, (2015) presents a numerical modelling approach for both static and dynamic modelling of track superstructure and vehicle-track interaction in various conditions such as light and conventional lines to heavy haul lines. He has modelled the sub structure and super structure separately and then coupled using stiffness parameters. The relationship between the deformation and the stress of each layer of the track

substructure was determined at each section and used for the dynamic analysis using multi body simulation tool.

Some researchers have used train as a multibody system (François et al., 2012) and evaluated the effects of vehicle's structural modification on numerical prediction results. Auersch, (2010) developed a simplified prediction model with soil-structure interface to predict the level of vibration in building and found that the consequences of resonance is moderate and observed to decrease in high frequencies. Simplified models provide limitations on structure and materials. When they cannot be obeyed, 3D models will provide results to desired level of accuracy. Much consideration is given to the loading type as it generates direct impact on model results. Unlike the early prediction models, Sheng et al., (2004) used point loads to predict the impact of train loads and justified the results are accurate compared to the actual results.

Lopes et al.,(2016) presents the experimental validation for a previously proposed numerical prediction model to predict the vibration inside the building due to railway traffic inside the tunnels. This takes serious concerns when dealing with historical buildings and monuments, precise equipment manufacturers, nano technology laboratories etc.

A. Sayeed & Shahin,(2016) presents a 3D FE model technique to assess the dynamic behaviour of the ballasted railway track during the movement of high-speed trains (HST). The critical velocity of various train-track-ground system was found, and the simulation result was presented in terms on coefficient of dynamic amplification of sleeper deflection vs speed which is combined to produce sensitivity charts to determine the critical speed for specific train track ground system.

Deformability of soil is one of the key components in FE analysis and can be modelled in various ways. Significantly different results are given for the models accounting for finite dimensions of the soil rather than the models considering spring and dashpot systems. Infinite soil doesn't have eigen mode. But practically the soft soils bounded by the rocks have eigen modes. Dynamic loading of a finite soil layer can cause resonance (Pap & Kollár, 2018).

Soil modelling is always critical in railway modelling as there is a need to combine both rail-track structure and soil structure. Different theories have been followed in adapting suitable techniques in rail-track-soil modelling. Boundary element method (BEM) is one such widely used method for its innate ability to replicate infinite domain and higher computational efficiency in frequency domain (Do Rêgo Silva, 1994). However, this cannot be used for complex geometries and non-linear problems as frequency domain is limited for linear problems.

Connolly et al.,(2013) generated a three-dimensional numerical model to analyse the intensity of ground borne vibration propagation induced by high speed railways at various distances on diverse embankment constituent materials. Elongated spherical geometry with absorbing boundary condition at the truncated boundaries is especially used for the soil modelling to increase the boundary absorption performance and unbounded nature of soil.

The numerical simulations of Dijckmans et al., (2015) investigate the effect of retaining heavy masses near the track to mitigate the vibration intensity. The results of the 2.5D numerical analysis concludes that the vibration reduction is independent of the distance behind the heavy mass for homogenous soil type and it strongly decreases with the increasing distance for the layered soil type.

2.3.3 Track modelling

Complexity of track modelling is very high due to the need to model various wave fields generated by the three-dimensional track components. Earlier models considered the structure in a two-dimensional plane along the track and assumed that the vertical loading is the dominant factor in wave propagation(G. Kouroussis et al., 2014). However, track modelling can be achieved assuming that the rail is continuously or discretely supported to the system. Behaviour of sleepers is neglected in continuously supported system assuming minimal participation to the overall track behaviour. The rail is discretely supported by sleepers and rail pads in discretely supported system by accounting all the possible effects.

Although conventionally rail beam is modelled as Euler beam, Grassie et al (Grassie et al., 1982) stated that this method is vague within the frequency range 50-1500 Hz and suggested advanced modelling technique using Timoshenko beams. However, the deviation of the results is negligible within the frequency range of 500 Hz. Also, Grassie et al., (1982), stated that the track resting on an elastic medium is simply satisfactory for the excitation up to 100Hz.

2.3.4 Track-soil modelling

Railway vibration can be categorized as static vibration and dynamic vibration depending on the way it originates. Static vibration is generated by the load and dynamic vibration is generated because of wheel-rail-soil interaction and unevenness. Hence, soil should be modelled carefully for accurate results. Soil is a non-homogenous substance consisting of solid granules, air, and water. The composition of soil structure heavily affects the vibration generation and propagation. Hence, non-linear behaviour of soil can be neglected if the shear strain is below 10^{-5} as in the case of railway vibration generation(G. Kouroussis et al., 2014). Hence, soil can be modelled as a homogenous structure.

2.4 Parameters influencing the railway vibration intensity.

The level of vibration observed at a building or site may vary due to various reasons such as distance to the road, train load, speed of the train, track parameters, and soil parameters and the response of the building depends on the structural parameters and type of foundation (Romero & Galvin, 2013).

Various components of body-wheel-track-ground system excite various frequencies depending on their physical and material properties. The wheel dynamics exciting low frequencies efficiently gets transferred to the ground when excited in wheel-rail natural modes. The high frequencies over 150 Hz produced by the rolling noise of wheel/rail system produces high vibration as the ground efficiently absorbs them because of its material and geometrical damping abilities. Figure 2.2 shows the frequency of vibration generated by various train-track components (D. P. Connolly et al., 2014).

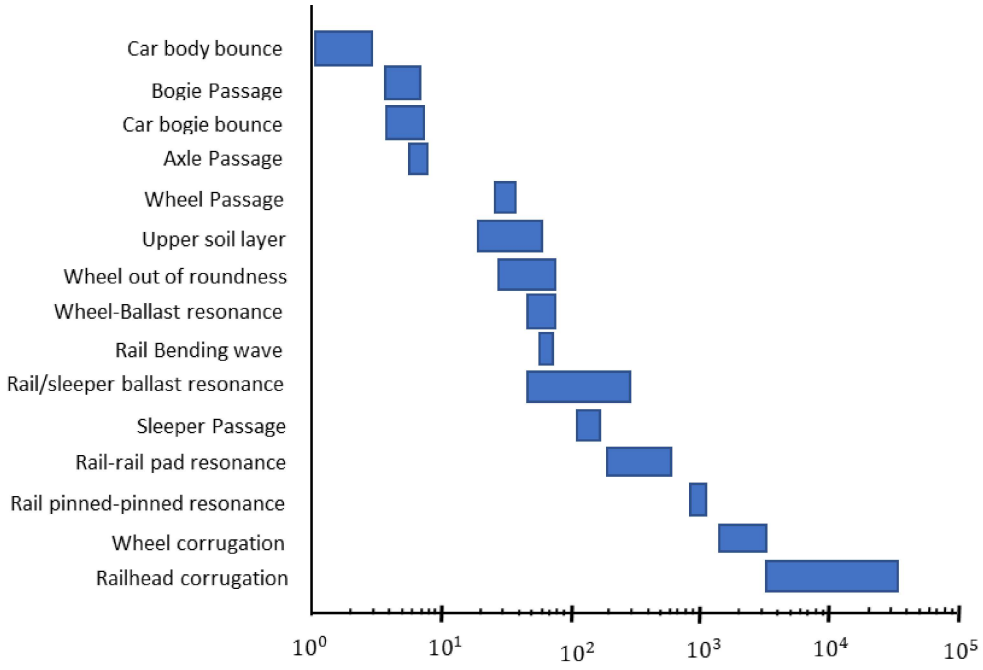

Figure 2.2: Main contribution of dynamic vehicle/track and soil interactions

The vibration levels are merely a function of the forces exerted by the vehicle on the ground. Hence careful attention should be given to the vehicle parameters during the study (G. Kouroussis et al., 2014). The vehicular forces may also arise from the irregularities at the wheel – rail interface. For any dynamic analysis, the FE size, boundary conditions and time steps have to be carefully chosen for accurate results (Galavi & Brinkgreve, 2014).

Considering the complex definition and description for all the parameters affecting the model simulation of the railway track system, has enhanced the performance of railway systems for obtaining high comfort and safety (Iwnicki, 2006). Krylov (1994) has considered the effects of all sleepers subjected to wheel action into the theory of generation of railway vibration. He has focused on the effects of induced vibration by superfast trains whose speed is greater than the Reileigh wave and the methods to suppress is discussed.

Swedish Rail Administration started X-2000 passenger HST service in 1997 along the west coastline between Goteborg and Malmo. Soon after the commencement, excessive vibration in the embankment was observed at Ledsgard site with soft soil ground condition. The investigations revealed the cause as critical speed, and the authorities reduced the functioning speed immediately (Woldringh & New, 1999).

The train-track-soil system is rarely analysed completely due to its complexity. Numerous theories applicable in this genre allows number of researchers to approach the problem in thousands of ways. Vibration mitigation methods have been analysed by Maldonado et al. (2017) in low frequency range using prediction models and foreseen their efficiency in higher frequency vibration levels. Georges Kouroussis et al., (2012) analysed T2000 trams circulated in Brussels due to numerous complaints received on its performance. The research findings on vehicle effects on ground is considered as one of the major findings.

2.5 Noise and vibration

The vibration generated by each cause has the potential to leave a negative impact on environment, especially on human and sensitive equipment. Feelable vibration and structural vibration are two ways of human impact. It can shake the building causing indoor noise. This is crucial in underground trains where the airborne noise is absence. For the delicate equipment, the impact on the buildings they rely on matters because even a small change makes huge difference.

To be precise, noise and vibration are two completely different things. The level of exposure and annoyance will vary among both. Ögren et al., (2017) compared the vibration exposure to noise exposure to find when the noise exposure is equally annoying as vibration exposure. A questionnaire was filled among the residents with and without vibration exposure and found that the noise level and vibration velocity have equal chances of causing annoyance.

Okumura, K and Kuno, K (Okumura & Kuno, 1991) carried out regression analysis of railway noise and vibration using the data from 79 sites along 8 urban railway

lines. From the study they concluded that the speed is the dominant factor contributing to the noise and the length of the train contributes the least.

Li et al., (2016) carried out an experimental analysis to find the ground borne vibration induced by subway vehicles and radiated noise in buildings. Initial assessment was done in the frequency range of 1-300 Hz and partial coherence function was used to distinguish the data. Using this methodology, various sources contributing to noise and vibration was found which helped to identify the dominant frequency of the ground borne noise is between 20~310 Hz.

Vithrana et al., (2013) carried out the investigation on identifying the level of awareness of workers on the risks associated with the construction activities, noise and vibration in construction sites and effect of noise and vibration on health of the workers. The Relative Importance Index (RII) of exposure to noise and exposure to vibration were found to be critical and concluded that the continuous exposure will adversely impact the worker's health.

2.6 Effects of vibration

2.6.1 On buildings

The induced vibration can cause severe and non-severe problems on buildings depending on their vibration intensity and the structural performance of the building. Factors such as the construction material of the building, foundation type, soil type etc influence of the structure's response to vibration (Jik Lee & Griffin, 2013). Effects such as shaking and micro cracks can be initiated even without the knowingly and could create enormous hazards even destruction when exposed to prolonged vibration.

The speed of Rayleigh waves is critical parameter in deciding the vibration intensity. Tremendous increase in the vibration level in association with critical speed is not only an environmental hazard. It can create numerous hazardous effects such as train derailment, operational issues, degradation of track foundation and interruption of power supply(Madshus & Kaynia, 2000).

2.6.2 On human beings

Vibration can create physical, physiological and psychological effects on humans(Jik Lee & Griffin, 2013). Generally, the level of threshold to vibrations varies from individual to individual. It also depends on the circumstance and is hard to exactly identify the general annoyance level as it varies from one to another. BS 6472, (2008) presents a guide to evaluate the level of human exposure to vibration in buildings.

For every individual there is a threshold limitation to noise and vibration. The people may not know the intensity or could tolerate until the limit exceeds the threshold limit. Longinow & Mohammadi, (2023) states that the threshold level purely depends on the level of expectation and one's confidence in safety can literally enhance the threshold.

Although the construction industry is one of the high-risk industries, the workers associated with the industry are less aware of it. Vithrana et al., (2013) concluded from his study that the long-term exposure could cause physical damage to human hearing, work related stress, and voice disorders.

2.7 Summary

This literature review provides a comprehensive overview of the broad field of railway vibration and its effects, offering a concise understanding of key aspects. The review encompasses topics such as vibration generation and propagation, highlighting both conventional and contemporary techniques used for vibration assessment, including experimental methods and computer software simulations. The review also touches upon theoretically proven techniques employed by researchers to enhance the accuracy and precision of FE models. Additionally, the study explores the impact of noise and vibration on structures and human beings, shedding light on their effects. Overall, this literature review presents a condensed yet informative account of railway vibration and its implications.

3. METHODOLOGY

3.1 Introduction

This research employed a combination of experimental and numerical analyses to examine the effects of train movements on the ground. The experimental study began with the collection of primary data and identification of parameters related to the existing conditions. It then proceeded to perform actual vibration measurements on-site. The objective of the experimental analysis was achieved through the development of a vibration sensing gadget called "VIBSEN". In parallel, a computer-based numerical FE prediction model was created using the MIDAS GTS NX FE software package. This model aimed to assess the ground vibration resulting from moving trains. To validate the FE prediction model, two approaches were adopted:

- Comparative analysis with the experimental data presented in the literature (Degrande & Schillemans, 2001)
- Comparative analysis with the experimental data obtained from this research (Thadsanamoorthy & Damruwan, 2020)

Additionally, a parametric study was conducted to explore the response of the train-track-soil system under various changing parameters. This chapter provides a detailed explanation of the procedures undertaken during these tasks.

3.2 Development of VIBSEN device

The measurement of vibration intensity is typically carried out using a Vibrometer. However, due to limited availability of multiple vibrometers in the laboratory, an electronic device was developed to sense vibration intensity using highly sensitive accelerometers. Among the options of High gravity type and Low gravity type accelerometers, the Low gravity MEMS accelerometer was selected, which operates based on the capacitance method. Various low gravity sensors were analysed, and the most suitable option was chosen based on considerations of efficiency, sensitivity, and cost-effectiveness.

3.2.1 Components of the accelerometer and functions

STEVAL-MKI180V1 sensor: This capacitive accelerometer functions under the principle of gravity. A seismic mass was suspended on one end of the spring while the other end was attached to the capacitor plate. The mass moves according to the force acting on the capacitor plate, thus changing the distance between the plate and mass. The change in the distance induces capacitance. The acceleration was measured according to the change in the capacitance.

The STEVAL accelerometer sensor has lots of advantages. Being able to mount on a Printed Circuit Board (PCB) is one of the biggest pros. Its sensing ranges between $\pm 2.5g$ and sensitivity is 0.076 mg/Digit. The features as per the STEVAL-MKI180V1 data sheet (Technical guide, 2017) follows:

Features:

- Complete LIS3DHH pinout for a standard DIL 24 socket
- Fully compatible with the STEVAL-MKI109V2 and STEVAL-MKI109V3 motherboards
- RoHS (Restriction of Hazardous Substances) compliant

Raspberry Pi: This is simply a minicomputer on palm; a small gadget that includes all the functions of a modern computer. Raspberry Pi 4 model B which belongs to the 4^{th} generation of the type was used in this study. This model was launched in June 2019, holding advanced features. Main idea of choosing this component was efficient usage at present and for further modification in future. The advanced features incorporated in this model are listed below:

Hardware:

- Quad core 64-bit ARM-Cortex A72 running at 1.5GHz
- 4GB LPDDR4 Ram options
- H.265 (HEVC) hardware decode (up to 4Kp60)
- H.264 hardware decode (up to 1080p60)

- Video Core VI 3D Graphics
- Dual HDMI display output up to 4Kp60

Interfaces:

- 802.11 b/g/n/ac wireless LAN
- Bluetooth 5.0 with BLE
- SD card
- 2 micro-HDMI ports supporting dual display
- 2 USB2 ports
- 2 USB3 ports
- 1 Gigabit ethernet port
- Raspberry Pi camera port
- Raspberry Pi display port

Software:

- ARMv8 Instruction set
- Mature Linux software stack
- Actively developed and maintained
    - Recent Linux kernel support
    - Many drivers upstreamed
    - Stable and well supported userland
    - Availability of GPU functions using standard APIs

Power supply: The Raspberry Pi 4 Model B requires good quality power supply of 5V at 3A. Permanent damage can occur with the extreme power supply.

ESP 8266: This is a low-cost Wi-Fi module with built-in network which enables the micro controllers to be connected to the Wi-Fi network and access the data from any place.

Vero board: This is a printed circuit board material of copper strips on an insulated paper board which contains numerous rows of holes in it. This helps the electronic components to be soldered for the circuit.

Voltage converter: This was used to convert the voltage of given power to 5V which is the functioning voltage of Raspberry Pi

3.2.2 Functionality of the VIBSEN device

The sensor data was transferred to the ESP8266 which was soldered to the Vero board where the sensor was also soldered. The USB cable attached to the ESP8266 transfers the data to Raspberry Pi and saves it there in a .txt file format. The Raspberry Pi can be supplied with the power for its functioning via many ways. The power bank was connected to the Raspberry Pi through a C-type USP cable. In case of a general power supply, the voltage converter should be used to provide the adequate voltage supply. The stored data was accessed from the Raspberry Pi interface using MobaXterm_Personal_21.2. The interface requires both the PC and the device to be connected to the same Wi-Fi network and the input of device IP address is needed for the access. Figure 3.1 shows the VIBSEN device developed in this study for the field measurements.

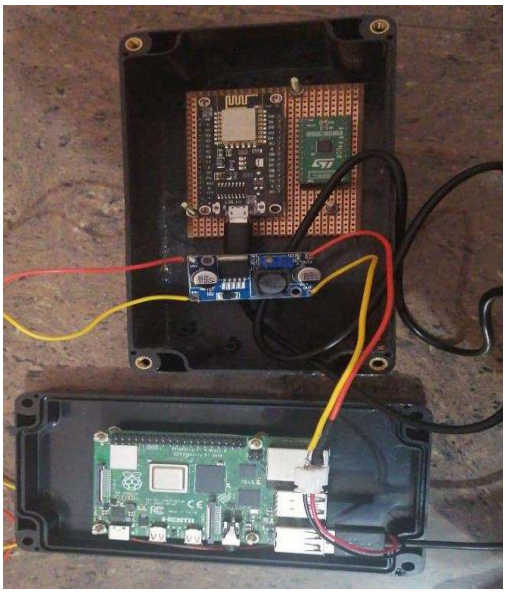

Figure 3.1: VIBSEN device

The ".txt" file of the receiving data was saved with the name of its created date and time. Device sampling rate was limited to 250 Hz due to the vanity to print faster. Hence, the file was renewed every 30 minutes to limit the file size. The saved file could be downloaded to the PC using "FileZilla" software. Figure 3.2 depicts the variations of acceleration-time history obtained at 3m from the centreline of the railway in all three directions (x, y, and z) using the VIBSEN device.

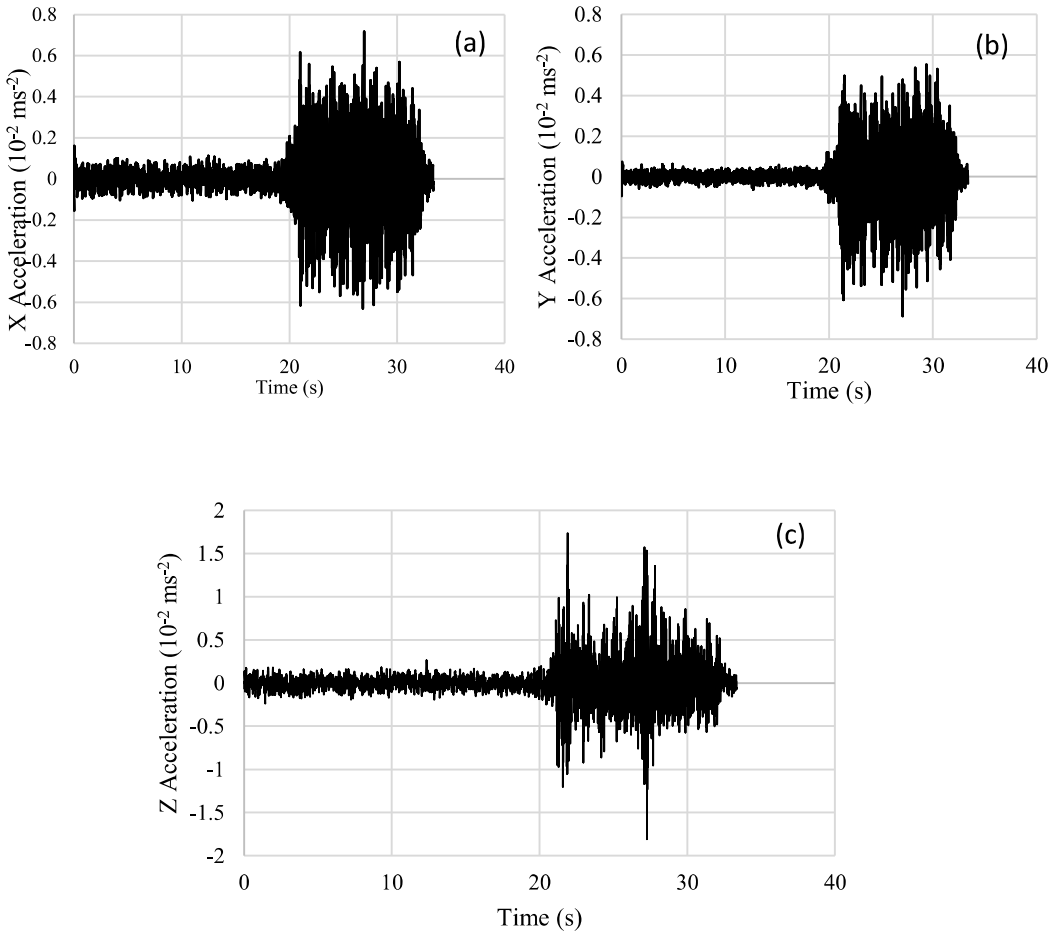

Figure 3.2: Acceleration along (a) X direction, (b) Y direction and (c) Z direction at 3m from the centerline of the railway track

3.3 Data analysis using MATLAB

The present study involved the analysis of the recorded raw data signal through the utilization of MATLAB software. To facilitate computational procedures, various

functionalities grounded in mathematical principles, including Fourier transform, convolution theorem and Laplace equation were employed.

The measured signal includes the noise caused due to the rail irregularities, movement of bogie components and other parts of the train, reduction gears, connecting wires and wind force together with the existing vibration level of the location. Filtering the forms of noise and vibration caused by other sources from the measured signal will provide the pure vibration signals induced by the train movements. MATLAB was used to extract the railway induced vibration signals from the school of measured signals. The signals were converted from time domain to frequency domain for easy analysis. Generally, the frequency range of train induced ground vibration is ranged between 40 Hz to 100 Hz (Heckl et al., 1996; Yang et al., 2018). Noise signals were filtered from the Fast Fourier transformed acceleration signals using low pass and high pass filters.

Denoising

The true signal of interest is always obscured by random unwanted variations called noise. Denoising techniques aim to enhance the quality and clarity of the signal by suppressing or filtering out the undesirable noise components.

In MATLAB the original signal of N samples is down sampled to a positive number which is less than floor ($log_2 N$). The noise signals are removed from the data using signal processing techniques like filtering, averaging and adaptive algorithms.

Low-pass filter

When a digital signal is passed through a low-pass filter, the signal below the cut-off frequency gets attenuated and the filtered signal possess reduced amount of noise intensity.

High-pass filter

High-pass filters attenuate the noise signals above the cut-off frequency and passes the signals below the cut-off frequency.

As the properties of railway vibration signals vary with parameters for each passage of train, the cut-off frequency for each dataset varies. Hence, trial and error method were used to identify the suitable cut-off frequency for each train type. Figure 3.3 shows the vertical acceleration-time history variation of the denoised signal at 3m from the centreline of the railway for the train moving at the speed of 18 m/s. Figures 3.4 and 3.5 show the vertical velocity-time history variation and vertical velocity-frequency variations obtained after processing the acceleration data.

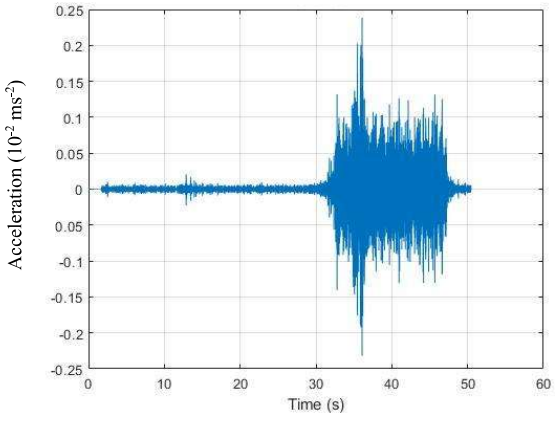

Figure 3.3: Vertical acceleration-time history variation

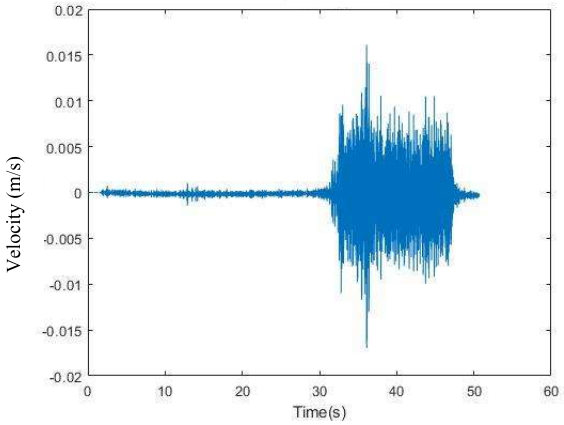

Figure 3.4: Vertical velocity-time history variation

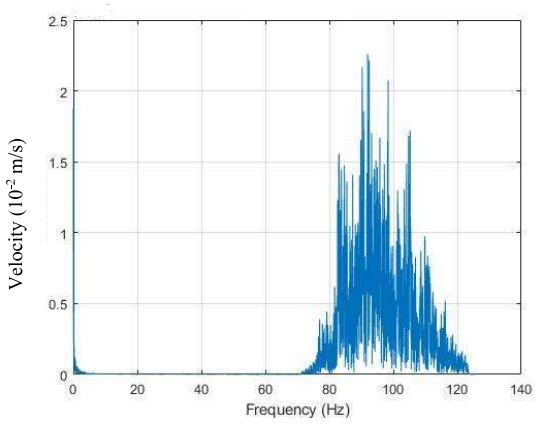

Figure 3.5: Vertical velocity-frequency history variation

The vertical velocity-frequency analysis for vibration induced by train travelling at 14 m/s at 3 m, 6 m, 9 m and 12 m are shown in Figure 3.6.

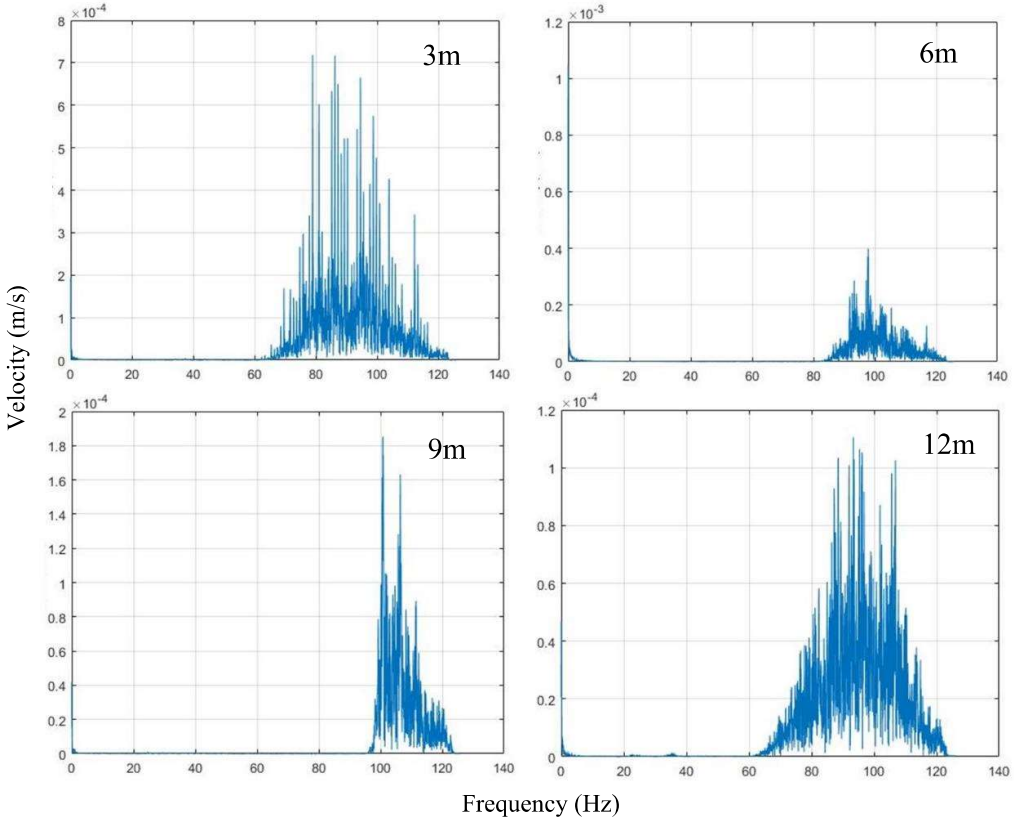

Figure 3.6: Vertical velocity - frequency analysis at 3 m, 6 m, 9 m, and 12 m

3.4 Field experimental analysis

3.4.1 Experimental location

The data for this experiment was collected besides the railway track between the Koralawala and Moratuwa railway stations near the Western coastal belt, at an isolated place with less vegetation. This surrounding was chosen and considered to be ideal for experiment as it is free from other sources of vibration such as road traffic, building construction and human activities. Figures 3.7 and 3.8 show the selected field location. The measurements were obtained during the early peak hours of the day throughout the month of July, during which no rain was observed. The experiment was conducted on a flat, stiff ground with sandy gravel soil type.

Figure 3.7: Experimental location view 1

Figure 3.8: Experimental location view 2

The number of data measured during a train passage was enormous, hence number of measurements made was controlled to reduce the complexity of analysis and storage. However, it became possible to store the bundle of data in a small chip due to the usage of Raspberry Pi, making the analysis and processing easier.

As railway induced vibration depends on uncountable number of influencing factors, controlling all of them is impossible in practical. Hence highly influencing factors were selected for the study. Apart from soil properties and vehicle properties, the moving speed of train was measured for each set of measurements.

3.4.2 Field experimental setup

The topsoil of 50 mm was removed, and the developed VIBSEN device was kept on a flat ground and placed firmly without any relative motion, to sense the railway vibration accurately. The horizontal level of the ground was verified using a spirit level.

At first, the device was kept at 3m from the centreline of the railway track located towards the land side, and the others were kept at 3 m interval from it respectively as shown in Figure 3.9. The power was supplied using power bank throughout the entire experiment.

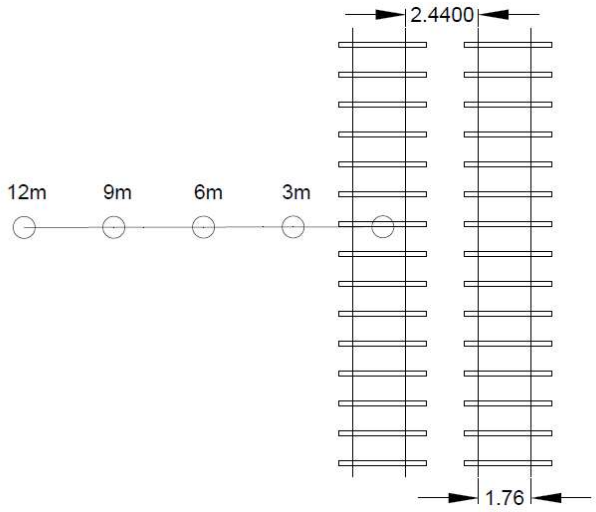

Figure 3.9: Plan view of the device location and railway track

3.4.3 Soil sampling and classification

Soil properties play a significant role in the monitoring of ground vibrations. The velocity, intensity, and attenuation of wave propagation are influenced by the characteristics of the soil. Therefore, a soil sample was extracted from the experimental site and brought to the laboratory for further analysis. Sieve analysis was conducted to determine the soil type. Figure 3.10 displays the collected soil sample from the field test location, while Table 3-1 and Figure 3.11 present the results obtained from the sieve analysis test.

Figure 3.10: Soil sample obtained from the test location.

Table 3-1: Sieve analysis test results of the soil sample

Sieve size (mm)	Mass of sieve (kg)	Mass of sieve +soil (kg)	Mass of soil retained (kg)	% Retained	Cumulative % retained	% Finer
4.75	0.8895	0.9740	0.0845	2.52	2.52	97.48
2.36	0.4810	0.5345	0.535	15.96	18.48	81.52
1.18	0.4380	0.5780	0.14	4.18	22.66	77.34
0.6	0.4100	0.8730	0.463	13.81	36.47	63.53
0.425	0.4565	1.25	0.7935	23.67	60.14	39.86
0.15	0.4120	1.6020	1.19	35.49	95.63	4.37
0.075	0.3880	0.5020	0.114	3.40	99.03	0.97
Pan	0.3645	0.3975	0.033	0.97	100	0

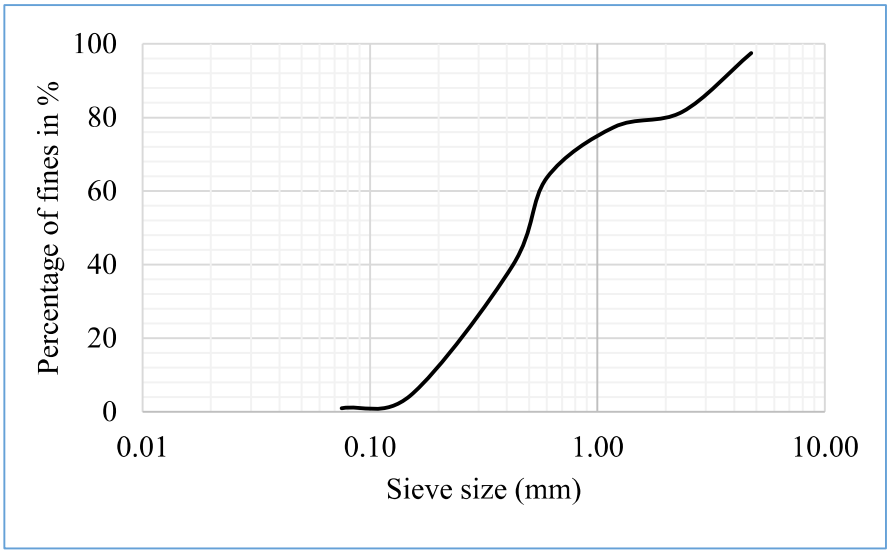

Figure 3.11: Particle size distribution of the soil sample

The borehole reports (refer to Annexure B) obtained in the vicinity of the field location were also consulted to gather additional information about the soil properties. These reports were referenced to supplement the understanding of the soil characteristics in this study.

3.4.4 Speed survey.

A specified distance of 100m was demarcated along the railway track, and the time taken by the train to traverse this distance was measured. Two individuals stationed at each end of the survey plot were responsible for the time measurement. Typically, train speeds in Sri Lanka range from 40 km/h to 80 km/h (11.1-22.2 m/s), depending on the train type and its intended purpose. In the case of the experimental location, being situated between two railway stations, the train's speed remained relatively constant, without any observed acceleration or deceleration.

3.4.5 Data acquisition and processing

The ground vibration induced by railway movements was measured in terms of acceleration by STEVAL-MKI180V1 triaxial accelerometer at a frequency of 250Hz and stored in Raspberry Pi. The Raspberry Pi was coded to start functioning when it is powered, and the data was saved in a file for every 30 minutes of time and a new file generates to record data. The data was analysed further using MATLAB software package.

3.4.6 Problems encountered in field experiment

Site location :

Even though, the site was chosen to avoid noise interruption to the maximum possible level, there were few interruptions observed. As the location is close to the seashore, where high wind intensity was observed even at the ground level. The 150mm of topsoil was removed and the device was placed below the ground level to avoid wind disturbances.

To minimize the disturbance from the residents near the test location, they were provided with a brief introduction regarding the research work being conducted. Data collection was scheduled during the peak hours on a working day to capture a larger volume of data. This time was chosen because trains tend to operate more frequently during this period, allowing for a higher frequency of data collection. By selecting this time frame, the research aimed to ensure an adequate representation of train movements and their corresponding vibrations.

Soil testing:

Collecting undisturbed sample form the ground was difficult because of the availability of ballast and hard rock particles in the ground. A proper soil sample was collected after few attempts and was taken for lab testing.

Speed survey:

As two people with stop watches were assigned to measure the time taken for the train passage, the level of accuracy is unpredictable. However, high attention was paid to derive accurate results.

Data collection:

Even though the vibration signals were recorded with 250Hz frequency range, the data measured per second was not constant and very high acceleration were observed at some points. The unrealistic values were considered to be errors and removed from the measured signal.

Data analysis:

Identifying exact cut-off frequency is difficult and hence only a much closer value was obtained. As trial-and-error method was used to identify the cutoff frequency, most convincing value was chosen for filtering, and this may deviate from the actual cutoff frequency.

3.5 FE modelling using MIDAS GTS NX software package

3.5.1 Coupled model

The three-dimensional (3D) FE model was developed using MIDAS GTS NX software to evaluate the behaviour of soil and track due to dynamic railway load. The vehicle dynamic load was coupled with the track- ground FE model of length 170m, width 19.1m and height 2m. The ground profile is extended in one side of the track with truncated boundaries on all sides of the model. All the components such as rail, sleepers, ballast layer, sub ballast layer and the subgrade layer were connected to each other based on Boolean theory. The model was divided into three sections, with the middle section of 10m being finely meshed to predict results with lower computational time. The front and end sections, on the other hand, were coarsely meshed as their primary purpose was to assess the vibration intensity of the approaching and departing vehicles. This approach allowed for an efficient balance between accuracy and computational resources, focusing computational efforts on

the critical middle section while still capturing relevant information from the surrounding areas.

The individual material properties of every component were considered in this study and non-homogeneous properties were carefully modelled and allowed to perform according to their own behavioural pattern. Figure 3.12 show the details of FE model.

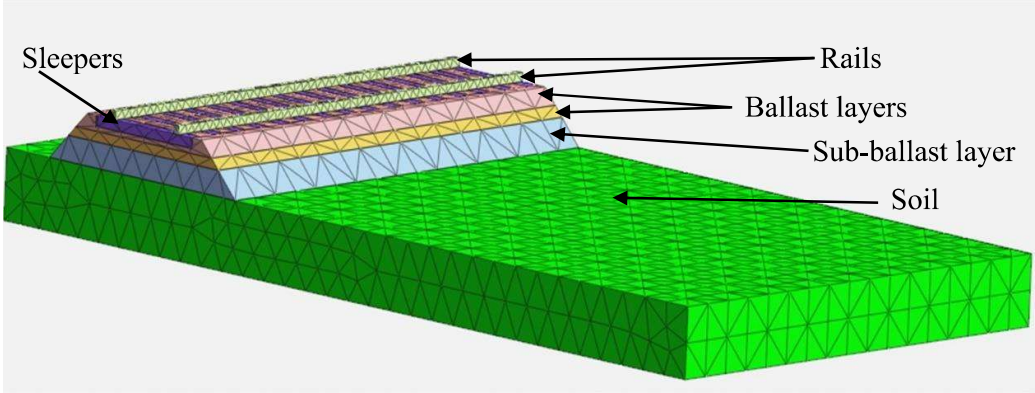

Figure 3.12: Fine meshed segment used for detailed analysis

3.5.2 The components of the FE model

The rail:

The rail was modelled as a non-porous material having a linear elastic behaviour. 3D solid elements having width and height representing the actual structure were used in modelling the rails.

The experimental location consists of concrete sleepers of dimension 0.16m width, 0.15m height and 2.1m length with 0.65m spacing. Hence, the same dimensions had been used in the FE model to replicate the actual scenario. The behaviour of concrete sleepers obeys the linear elastic theory. Hence, the same principle was used in the FE model.

Ballast and sub ballast:

Ballast and sub-ballast layers were modelled as solid blocks with material properties recommended in the literature (Degrande & Schillemans, 2001). After prudent study of the behaviour of ballast and sub-ballast layers, hardening soil model was used for the simulation in the FE model.

Subgrade:

The soil is an anisotropic material which does not behave equally in every direction. Therefore, modelling of soil varies depending on the assumptions made in the analysis. In this 3D FE model, soil was modelled to behave based on the principles of Mohr-Coulomb law. This represents the first order effects of the soil model and requires the input of five parameters for in cooperating elastic and plastic behaviour. Elastic modulus and Poisson ratio are required to replicate the elastic behaviour while dilatancy angle, cohesion factor and friction angle were used to simulate the plastic behaviour.

3.5.3 Elements, nodes, and mesh size

Eight nodal auto meshing technique was used in FE model to ensure the proper connectivity between layers and to transfer vibration effects. Mesh size was selected to allow surface waves with minimum wavelength to propagate through the medium. It depends on the velocity of waves in the corresponding medium and minimum wavelength. Finer the mesh, accurate the results and higher the computational time. The number of equations is directly influenced by the number of nodes of the system. Therefore, optimum mesh size was chosen for each material type, considering the wave velocity in that respective medium. The wave velocity used in this study is given in Table 3-2.

Table 3-2: Primary and Secondary wave velocity of soil

Type of soil	Type of wave	General range of Velocity(m/s)	Velocity (m/s)
Soft clay	Primary wave	200-800	270
	Secondary wave	100-1500	175
Dense Sand	Primary wave	500-1200	550
	Secondary wave	100-300	300
Hard Clay	Primary wave	800-2000	940
	Secondary wave	200-800	598
Gravel	Primary wave	300-2000	425
	Secondary wave	200-1000	350

Source: Kokusho Takeji & Yoshida Yasuo, (1997); Georges Kouroussis et al., (2016); Kulkarni et al., (2010)

3.5.4 Vehicular load and load distribution

The train body load during service condition together with the bogie and wheel load were combined to axle loads and assigned on a nodal path to move in a specific speed for a duration. The direction of passage was activated by providing a start node and end node in the selected path of nodes. Axle nodes at distances from the first axle (origin 0,0) in gravity direction were fed in the model to enable dynamic loading.

The default train types such as KTX 8 cars and KTX 6 cars of Korea are readily available with the axle load and distances together with the user editing option. The simulation of train movement under Sri Lankan context was done by using a speed of about 60km/h (16.6 m/s), whereas validation of experimental work of Degrande & Schillemans, (2001) was done using the speed of 314km/h (87.2 m/s).

3.5.5 Damping

In the FE prediction model, the level of damping of the system was controlled by the damping ratio and each material was modelled according to its specific damping parameter. Degrande & Schillemans (2001) suggested a damping ratio of 0.03 for the soil condition of his experimental location. The same value was used for the Sri Lankan experimental location as both soil conditions are similar.

3.5.6 Boundary condition

Transmission of induced vibration through wave forms occurs in rail-track-soil system. Two stages of analysis required two different boundary conditions depending on their peculiar needs. Ground surface spring was used during eigen value analysis and viscous boundary was used at the truncated boundaries in dynamic analysis to prevent wave reflection back to the system. The induced waves were allowed to propagate through the truncated boundaries without reflecting into the system. The Equations 1-4 were used to calculate the input damper value according to the ground material.

For the Primary wave, $C_p = \rho A \sqrt{\frac{\lambda+2G}{\rho}}$ (1)

For the Secondary wave, $C_s = \rho A \sqrt{\frac{G}{\rho}}$ (2)

$$\lambda = \frac{vE}{(1+v)(1-2v)} \quad (3)$$

$$G = \frac{E}{2(1+v)}, \quad (4)$$

Here, E is the elastic modulus, v is the poisson ratio, ρ is the density, C_p is the speed of the primary wave, C_s is the speed of the secondary wave and A is the area.

3.5.7 Material properties for FE model

Most of the material properties that were used in this study were derived from the literature apart from those of the soil at the site which were determined based on the

data obtained from the laboratory testing. Table 3-3 shows the material properties that have been used in the FE analysis.

Table 3-3: Material properties used in the FE analysis

Components	Properties
Rail	Type - UIC 60 Material model = Linear elastic Damping – 0.01 I=0.03038× $10^{-4}m^4$ Unit weight – 76.74 kNm^{-3} E = $210 \times 10^3 MPa$ Poisson Ratio = 0.3 Material type – Non-porous
Concrete sleeper	Material – Concrete Material model – Linear elastic Material type – Non-Porous E = 10× $10^6 kNm^2$ Poison ratio = 0.15 $\gamma - 20.148\ kg/m^3$
Ballast	Damping = 0.04 Material model = Hardening soil Material type = Drained $E_{50}^{ref} = 21{,}340\ kNm^{-2}$ $E_{oed}^{ref} = 21{,}340\ kNm^{-2}$ $E_{ur}^{ref} = 64{,}020\ kNm^{-2}$ Unit weight = 15.6kNm^{-3} Cohesion = 0 Friction angle = 58.47° Dilatancy angle = 12.95° Reference confining pressure = 50 kNm^{-2} Stress dependent stiffness factor = 0.5 Coefficient of earth pressure at rest for normal consolidation = 0.3 Failure load ratio = 0.9
Sub ballast	Material model = Mohr-coulomb Material type = Drained E = 80,000 kNm^{-2} Unit weight = 16.67 kNm^{-3} Poisson ratio = 0.35
Soil	Damping = 0.03 Unit weight = $\gamma = 18\ kN/m^3$ Poison ratio = 0.3 Cohesion = 0 Friction angle = 30° Dilatancy angle = 0°

Source : B. Indraratna et al., (2012), Degrande & Schillemans, (2001) and Khordehbinan, (2009).

3.5.8 Material behaviour

Rail and Concrete sleeper – Linear elastic behaviour:

The linear elastic material model is applicable to the materials which satisfies the following assumptions:

- The elastic strain should be very small.
- Can be isotropic, orthotropic, or fully anisotropic.
- Possesses temperature dependent properties or field variables.

Linear elasticity signifies the behaviour of solid elements' deformation and internal stress due to the applied loading. It mainly depends on two parameters: Young's modulus and Poisson's ratio which can be derived experimentally using uniaxial compression / tension test. Considerable amount of steel in rail beams and concrete behaviour in sleeper allow them to behave according to the principles of linear elasticity. After releasing the developed stress from the rail beam and sleeper, they return to original shape. MIDAS GTS NX provides facility to inculcate the exact behaviour using inbuilt material model whereas elastic modulus, Poisson ratio and unit weight are the input parameters.

Ballast – Behaviour of Hardening rock:

Ballast is one of the major components in the infrastructure of the rail-track-soil system. The tracks are laid on the compacted ballast layer which is placed above the roadbed. Even though, there are non-ballasted tracks, ballasted tracks are preferred for their well-known functionality.

The ballast bed increases the functional area of the system and reduces the stress on roadbed induced due to high train impact load. This reduces or prevents the track creep. The rolling of wheels on the rails produces horizontal thrust which drives the track to move with the sleeper. This action is prevented by installing ballast bed around sleepers which will resist the sideways movement.

Ballast layer is also preferred for its absorption property. When they are relatively softer than rail, fasteners and sleeper, the ballast layer prevents the damaging of track components from excess impact forces. High void ratio of ballast layer prevents the track from submerging during flood. It helps to drain the water and maintain the water table at low level.

Hardening model available in MIDAS GTS NX is used to exactly replicate the behaviour of ballast in 3D space. The total strain is calculated using the stress dependent stiffness parameters. This is more advanced than Mohr-Coulomb model. In Mohr-Coulomb model, limiting stress states are described in terms of phi, dilatancy angle, and cohesion. However, additionally three more parameters are used in HS model (Triaxial stiffness, Triaxial unloading stiffness and dependency of stiffness moduli).

Sub-ballast and soil – Mohr-Coulomb law:

The sub-ballast layer is laid in between ballast layer and soil layer which functions as a moist barrier as well as a supporting system to the entire track system. This helps to prevent the track from flooding and avoid any inconveniences due to raised water table. Hence, the sub ballast and soil layers have been modelled using Mohr-Coulomb law in order to allow for shear movements. MIDAS GTS NX software enhances the FE model by providing more realistic features for the FE model. Thus, the properties of cohesion, friction and dilatancy angle were considered in this Mohr-coulomb model.

3.6 Chapter Summary

This chapter briefed about the methodology carried out to fulfil the objectives in this research. The development of the vibration sensing device (VBISEN) through selection of components, assembling and programming procedure carried out in the experimental study were discussed. The development of the FE model, selection of material properties and assignment of boundary conditions were briefly explained. Additionally, a few other essential tests carried out to derive the train speed, soil parameters, and challenges faced during the experimental study were discussed.

4. RESULTS

4.1 Introduction

This chapter presents the results of the experimental study, Finite Element (FE) analysis and the parametric study conducted in this research. Experimental study was carried out by placing the VIBSEN devices at the relevant locations at the site. VIBSEN device was calibrated with the acceleration of gravity and was further validated with the readings obtained from the vibrometer.

FE analysis was carried out using the MIDAS GTS NX software package by incorporating train-track-ground system. The developed FE model was validated by comparing with the results obtained from the experimental study and those available in the literature. Finally, the results of the parametric study were presented in the thesis.

4.2 Gravity calibration of VIBSEN device

The higher accuracy of the measured results using the developed VIBSEN device was ensured by the used of highly sensitive STEVAL accelerometer sensors. In addition to that, gravity calibration was done to assess the dependability of the sensed acceleration and the VIBSEN device.

The device was placed on a flat horizontal surface and allowed to measure the acceleration in all three directions. The results (refer Figure 4.1) show that the acceleration in Z direction (vertical direction) is close to $9.81ms^{-1}$ which is the gravity acceleration, confirming the accuracy of the device in measuring the accelerations.

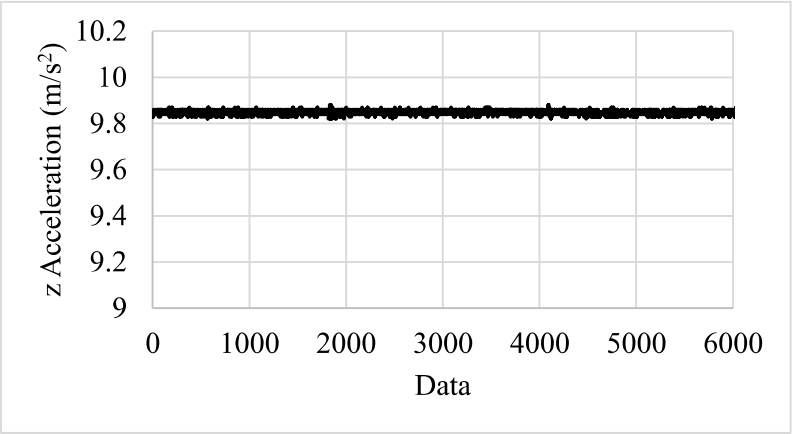

Figure 4.1: Vertical acceleration of the VIBSEN device

4.3 Calibration of VIBSEN device with vibrometer

Field experimental study was conducted using VIBSEN device together with calibrated vibrometer to analyse the suitability of the VIBSEN device. The data obtained from the five train passages has been presented in Table 4-1 and Figure 4.2.

Table 4-1: Calibration results of VIBSEN device and vibrometer

Speed of train (km/h)	VIBSEN PPV (mm/s)	Vibrometer PPV (mm/s)	% Deviation
63.8	16.098	16.02	0.48
38.9	5.13	5.281	-2.94
56.8	15.26	15.98	-4.71
77.7	17.588	17.64	-0.30
40.8	5.315	4.969	6.51

Overall, the readings obtained from the VIBSEN device agreed well with those obtained from the vibrometer, where the deviation of the readings lie in a range from 0 to ±7% which is acceptable. Both devices were placed sideby side assuring the same distance from the track. However, the soil properties and ground variation may be considered valid reasons for the minor changes in the results.

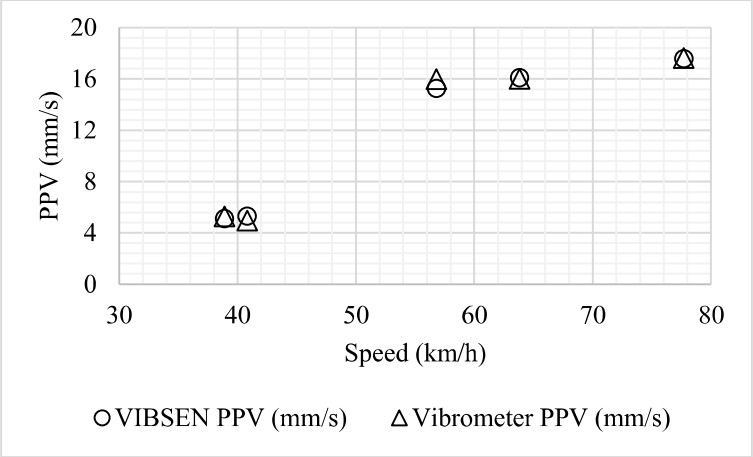

Figure 4.2: Measured data from VIBSEN device and vibrometer

4.4 Field Experimental results

The experiment was conducted at an isolated place close to the seashore located between Koralawella and Moratuwa railway stations ensuring the elimination of disturbance from other sources of vibration. Morning and evening peak hours were chosen to measure the data due to the higher number of railway passage. The data were measured and recorded by the VIBSEN device and signal processing was done using MATLAB as explained in the Chapter 3 of the thesis. Soil investigation and speed survey were done additionally to investigate the soil parameters and train speed respectively.

4.4.1 Soil investigation

The particle size distribution of the soil sample was obtained by conducting a dry sieve analysis test (refer Figure 4.3). The Equations 5-9 show the derivations from the particle size distribution and equations that were used to derive the grading characteristics of the soil. According to the Unified soil classification system (USCS), the soil sample obtained from the experimental location is classified as Poorly graded sandy soil. Borehole test reports at a location close to the experimental site have also been referred (refer Appendix B)

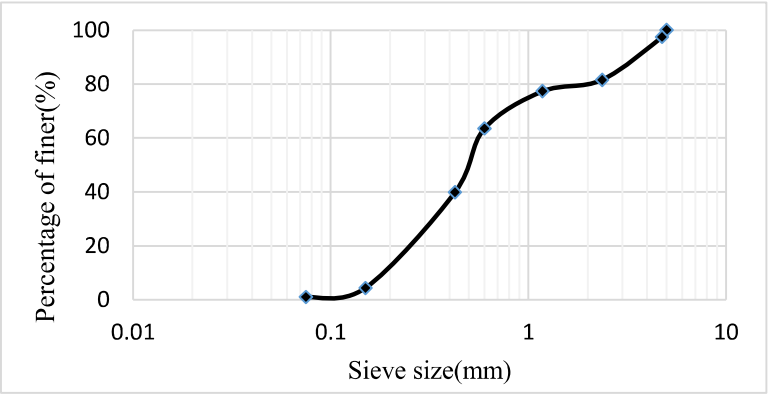

Figure 4.3 : Particle size distribution-Dry sieve analysis

From the graph in Fig 4.3,

- $D_{10} = 0.19$ (5)
- $D_{30} = 0.34$ (6)
- $D_{60} = 0.56$ (7)
- $Cc = \frac{{D_{30}}^2}{D_{60} \times D_{10}} = 1.086$ (8)
- $Cu = \frac{D_{60}}{D_{10}} = 2.95$ (9)

4.4.2 Experimental result of VIBSEN device for a train travelling with a speed of 63.7 km/h (17.7 m/s)

The vertical acceleration - time history variation at 3 m distance from railway centreline when a train travelling at a speed of 63.7 km/h (17.7 m/s) was obtained from the experiment and is shown in Figure 4.4. The average gravity acceleration has been deducted from the measured data and axis of acceleration is made zero for effortless visualization of the induced vibration. The graph states that from time 0 to 27 seconds, the vibration sensed by the device is close to zero. The acceleration increases gradually from 27th second and decreases after 47 seconds. The increase in the acceleration from 27-35 seconds states the approach of engine towards the location of data collection and the peak acceleration is obtained when the engine crosses the location of data measurement.

The ground acceleration induced by the influence of train engine is higher than that of the train bogies. The velocity-time history analysis of the induced vibration is obtained as a result of the Fourier analysis and presented in Figure 4.5.

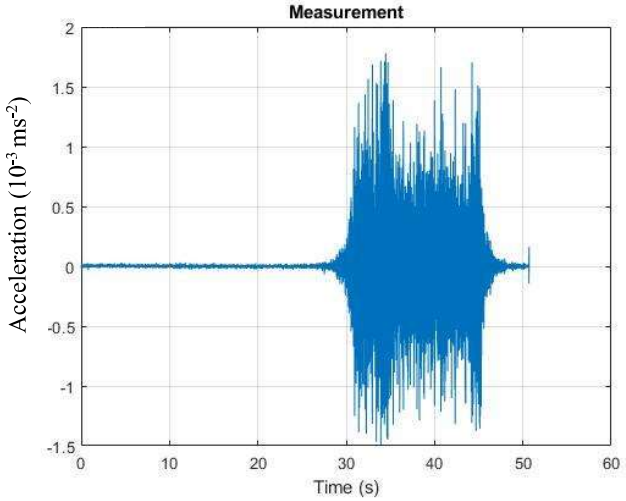

Figure 4.5 : Acceleration - time history variation for the train travelling at a speed of 63.7km/h (17.7 m/s)- VIBSEN device

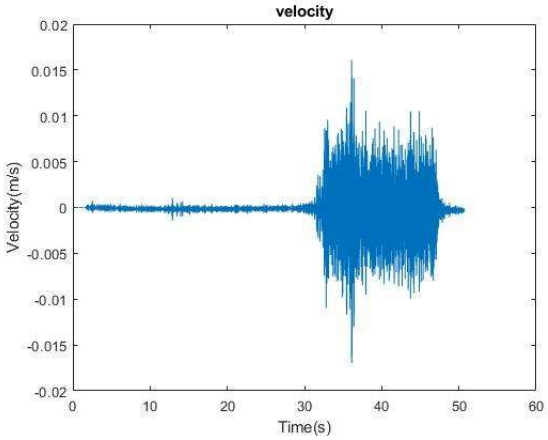

Figure 4.4: Vertical velocity-time history variation for the train travelling at a speed of 63.7km/h (17.7 m/s)

The passage of train lasted for 20 seconds, and the maximum intensity of 15 mm/s was observed when the engine crossed the location. The peaks were observed due to the passage of each axle. Even though, signal processing was done, there might be

noise signals still available in the data set by which there could be some deviations from the actual result.

4.4.3 Analysis of experimental data considering the speed of the train

Figure 4.6 shows the variation of the vertical PPV with the distance for 6 trains moving at different speeds. There is nearly an exponential variation of PPV with distance. Overall, it is evident that the trains with high speed show a greater intensity than those with less speed. However, the train travelled at a 68.8 km/h (19.1 m/s) velocity exhibits a high intensity than the train travelled at a 73.6 km/h (20.4 m/s) velocity. This may be due to the variation in the load, type of train and presence of irregularities.

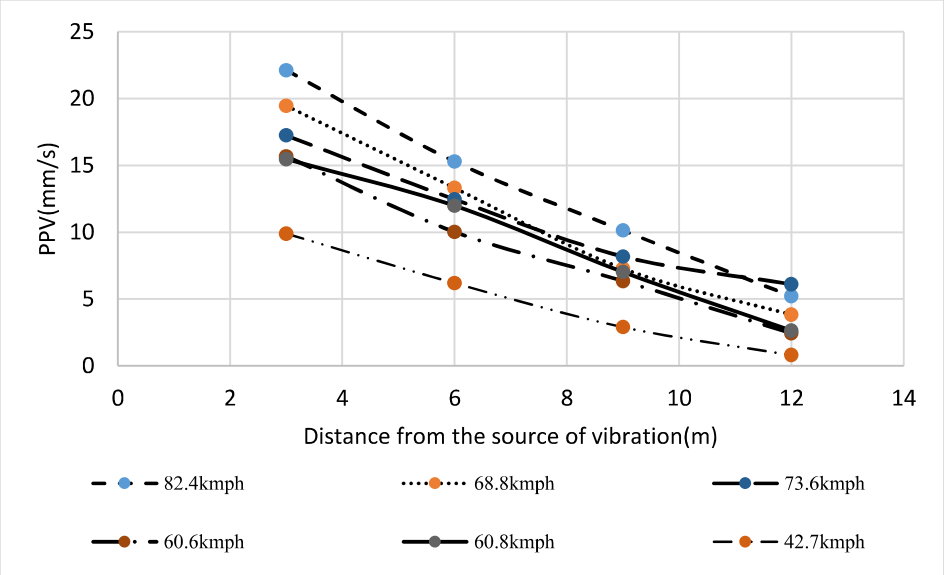

Figure 4.6: Variation of vertical PPV with the distance from the railway track

4.4.4 Analysis of the variation in vertical PPV when two trains cross at the same time

Table 4-2 displays the vertical PPVs obtained from the experiment at distances of 3m, 6 m, 9 m, and 12 m from the centreline of the 1st track under two scenarios: (a) when two trains cross simultaneously, and (b) when a single train passes at a high speed. As anticipated, despite the relatively lower speed of both trains, a significant impact occurs during their simultaneous passage. The PPV at a distance of 3m was

measured at 28.54 mm/s and exponentially decreased to 12.01 mm/s at 12m. In contrast, the train traveling at 82km/h only generated a PPV of 5.21 mm/s at 12m. Therefore, in addition to considering individual passages, it is crucial to account for the critical case of simultaneous train passage. The measured data is graphically presented in Figure 4.7.

Table 4-2: Vertical PPVs obtained from the experiment under two scenarios: (a) when two trains cross simultaneously, and (b) when a single train passes at a high speed

Case	Track no	From- To	Speed (km/h)	Speed (m/s)	PPV-3m	PPV-6m	PPV-9m	PPV-12m
(a)	2	M-G	67.24	18.7	28.54	22.38	16.36	12.01
	1	G-M	74.52	20.7				
(b)	1	G-M	82.38	22.9	22.12	15.28	10.12	5.21

Note - M-Moratuwa, G-Galle

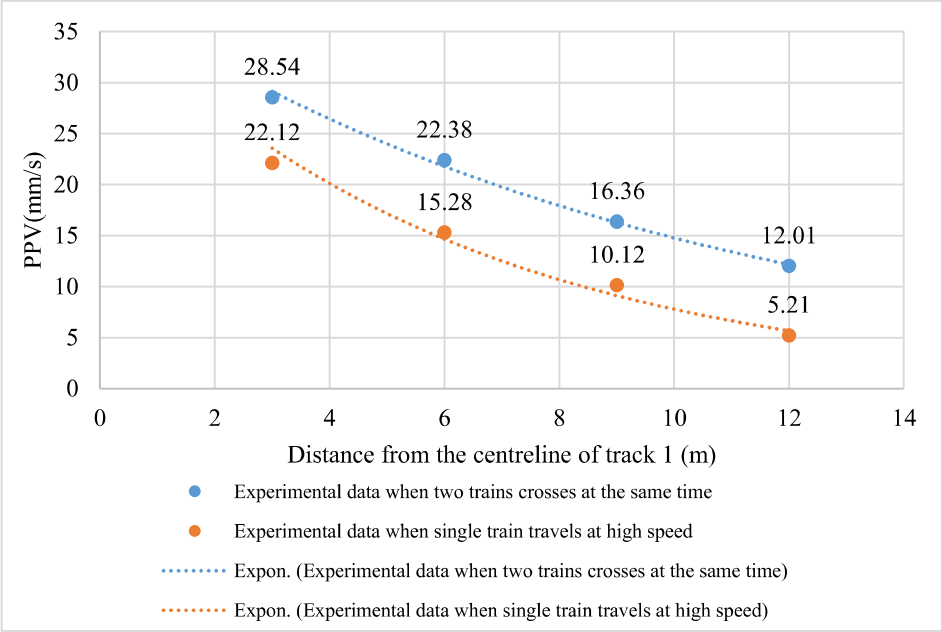

Figure 4.7: Variation of vertical PPV with distance under two scenarios

An exponential relationship between the vertical PPV and the distance from the railway track is described by Equation 10, which was derived from the graph,

assuming that the influence of all other variables at that specific location is negligible. This is considered critical compared to the generated vibration induced by the single train.

$$y = 38.959\, e^{-0.097x} \quad (10)$$

4.4.5 Identifying the safe distance using standard guidelines

The results of this study show that the PPV of free field vibration in the location of experiment has exponential variation with the distance. The threshold PPV of the structures is shown in Table 4-3.

Table 4-3: Maximum allowable vibration level for building types

Type of structure	Vibration - peak particle velocity (mm/s)			
	Foundation frequency			Plane of floor of upmost storey
	Less than 10 Hz	10 to 50 Hz	50 to 100 Hz	Frequency mixture
Buildings used for commercial purposes, industrial buildings, and similar designs	20	20 to 40	40 to 50	40
Dwellings and buildings of similar design and or use	5	5 to 15	15 to 20	15
Structures that, because of their sensitivity to vibration, do not correspond to those listed in lines 1 and 2 and are of great intrinsic value (eg buildings that are under a preservation order)	3	3 to 8	8 to 10	8

Source: German standards DIN4150-3

The measured frequency values on the ground varies from one train to the other. However, most of them lie above 50 Hz. Therefore, it is assumed that the building foundation frequency could be above 50 Hz as a worst case, neglecting the energyloss when transsfering vibration from ground to the foundation of the building.

The German standards DIN 4150-3 indicates that, the dwellings whose foundation frquency is between 50 Hz – 100 Hz must posses ppv between 15 to 20 mm/s to reduce the damages caused to the buildings. Hence, for a single storey dwelling, the allowable minimum ppv is 15 mm/s. According to Equation 10,

$$15\ mm/s = 38.959\ e^{-0.097x}$$

$$x = 9.839\ \text{m}$$

Here x is the transverse distance from the railway track in "meters (m)" and y is the ppv in "mm/s".

Therefore, when two trains cross simultaneously, the minimum safe distance is approximately 10 m from the centreline of the track. However, it is important to note that this event occurs rarely at a given location during a day. When considering the passage of a single train, the maximum safe distance is found to be approximately 6 m from the centreline of the track. It should be emphasized that these recommendations are specific to the soil profile present at the experimental site, and the minimum safe distances may vary depending on the subgrade soil type and its specific parameters.

4.5 Validation of the FE model

4.5.1 Comparison of field experimental results and FE simulation results.

Each of the VIBSEN devices was kept at 3 m distance starting from the centreline of the railway track along the perpendicular direction outwards the track. The vibration intensity of several moving trains was measured together with their speed data. The vibration intensity measured during the passage of the intercity train travelling at a speed of 18 m/s (64.8 km/h) from 4 ground locations (3 m, 6 m, 9 m and 12 m away from the centreline of track 1) are shown in the Figures 4.8-4.11. The same consequence was modelled using the MIDAS GTS NX software and FE simulation results obtained from the FE prediction model are compared with the experimental results.

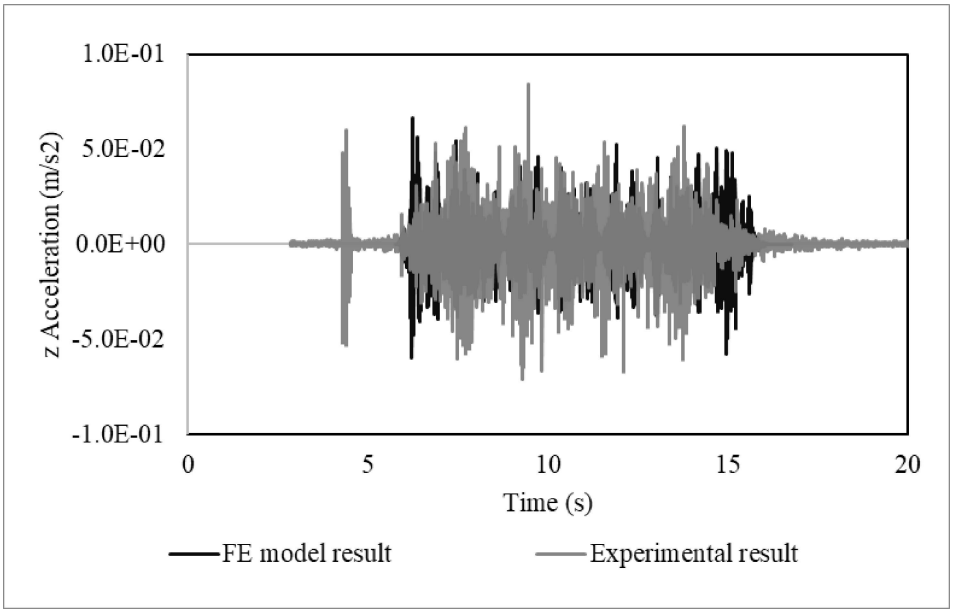

Figure 4.8 : Comparison of the acceleration-time history variation at 3 m

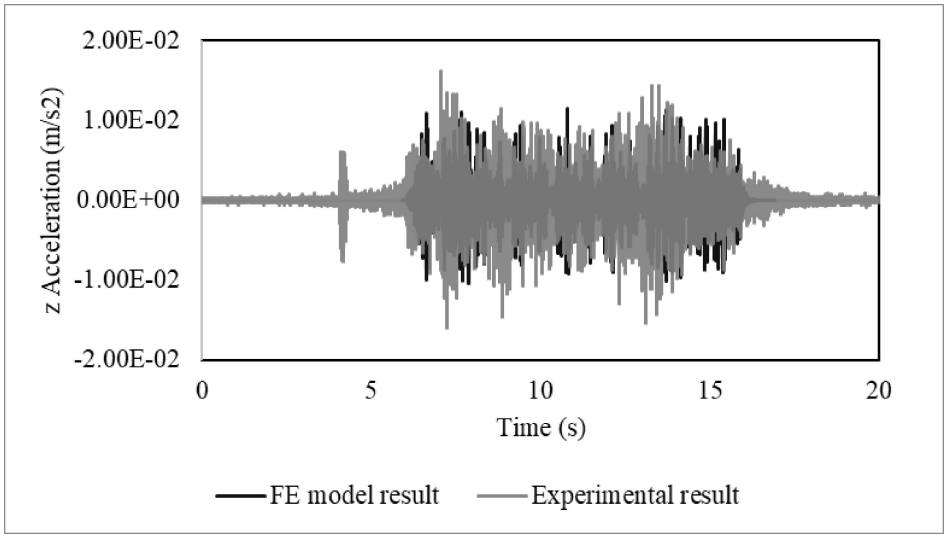

Figure 4.9: Comparison of the acceleration-time history variation at 6 m

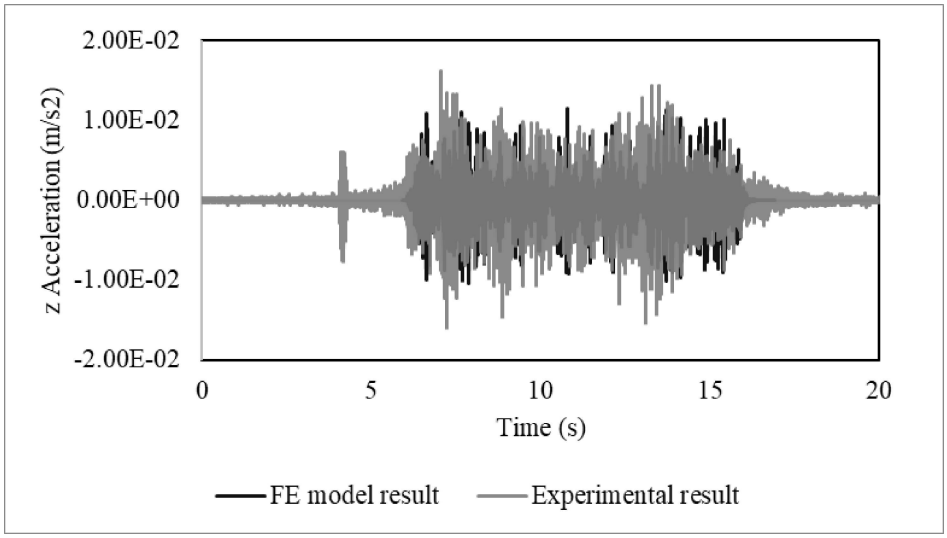

Figure 4.10: Comparison of the acceleration-time history variation at 9 m

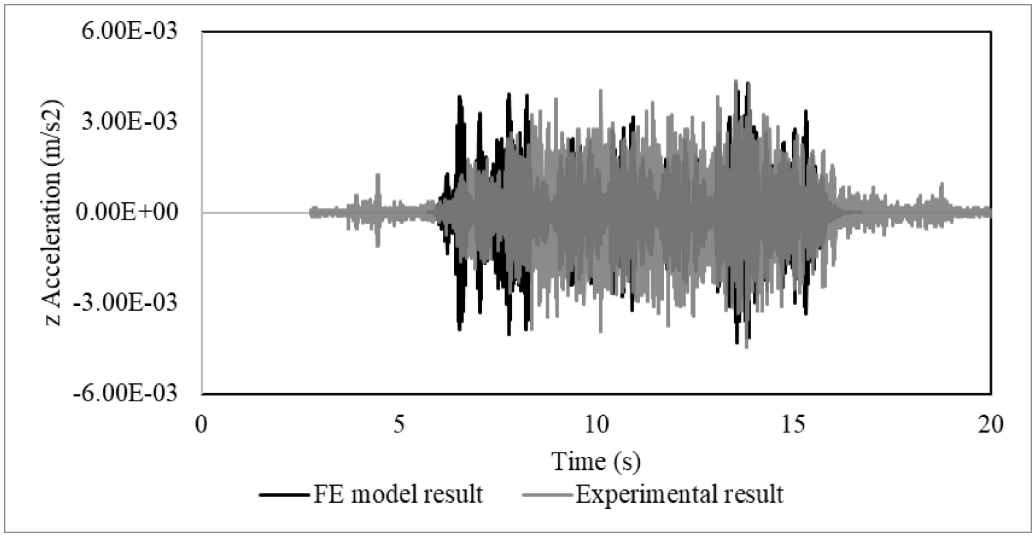

Figure 4.11: Comparison of the acceleration-time history variation at 12 m

Overall, it is evident that the acceleration-time history variations obtained from the FE model are agreed reasonably well with those obtained in the experiment at all four locations. A sudden peak in the intensity of the acceleration is observed in the experimental data at all the four locations. This is because of the whistle of the train. The air noise generated by the whistle, propagated through the air medium and sensed by the VIBSEN device resulted in the peak variation observed before the train reached the location. This ensures the sensitivity of the accelerometers and their accuracy. Apart from that, there are a few minor peaks observable in the graph. The non-uniform ground properties, excess vibration due to excess load impact etc. could be reasons for the minor deviation between both results. However, as a witness of the existing field condition, it is believed that the irregularity of the train-wheel-track system may be one of the reasons for the variation in the results.

4.5.2 Comparison of field Experimental results of Degrande & Schillemans (2001) with the FE simulation results.

The study of Degrande & Schillemans (2001) about the high-speed trains travelling between Brussels and Paris having the speed range of about 223 km/h to 314 km/h (61.9 - 87.2 m/s) were chosen particularly for the study of identifying the physical phenomenon of induced vibration during the passage of train. He placed 10 seismic

piezoelectric accelerometers mounted on Aluminium stakes at 10 locations and recorded the data at the sampling rate of 1000Hz. Though data sets of 5 varying train speeds have been produced, more time was spent on the study of Thalys HST travelling at the speed of 314 km/h (87.2 m/s). The vibration intensity at various locations were produced for easy comparison in both frequency and time domains.

The four locations (4 m, 6 m, 8 m and 12 m) were picked from the previous research work of Degrande and presented together with the FE prediction model simulation results for comparison. Figures 4.12-4.15 show the Vertical PPV - time history variation for the selected Thalys HST moving at a speed of 314 km/h (87.2 m/s) obtained from both field experiment and the FE model.

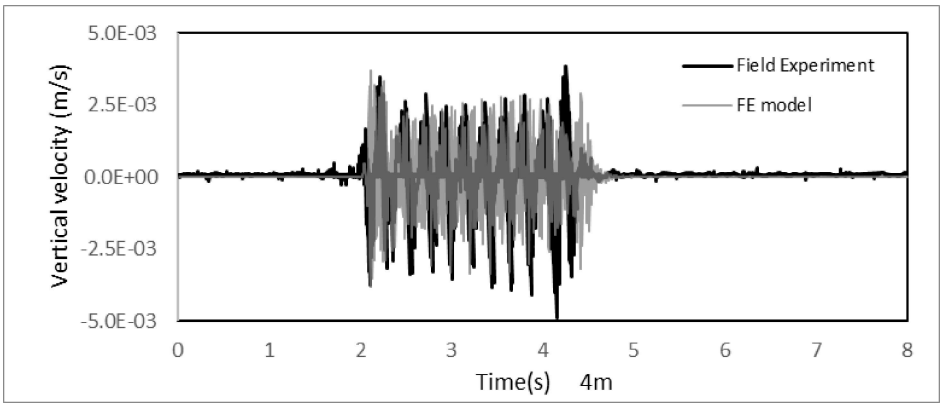

Figure 4.12: Comparison of Vertical PPV – time history variation at 4m

Figure 4.12 compares the variation of the Vertical PPV at a 4 m distance from the railway track, showcasing the results of the field experiment conducted by Degrande & Schillemans (2001) and the FE simulation results obtained from the present study, represented in two distinct shades. The data sets exhibit a high level of correlation, indicating a strong agreement between them. In the field measurements, there are some low-level pulsations observed before and after the passage of the train, which are likely attributed to the train noise and other external disturbances that are not present in the FE simulation. Notably, two sudden peaks, occurring in both positive and negative directions, are observed in the experimental results between the 4^{th} and 5^{th} seconds, which differ from the other measurements. These peaks could potentially be caused by irregularities on the track or wheels. It is unlikely that varying ground

conditions are responsible for this behaviour, as the entire measurement was conducted at the same location.

In contrast to the field data set obtained at 4m, the field data set at 6m distance, depicted in Figure 4.13, shows a slightly lower intensity than the predicted values. Upon analysing Figure 4.13, it becomes evident that both peaks consistently align with each other, generating intense vibrations. There is a minor deviation observed between the simulation results and the field data, which falls within an acceptable range with a safe margin. The highest observed deviation is 0.0001852 m/s, equivalent to 0.18 mm/s. This variation in the results could be attributed to factors such as the non-homogeneous properties of the soil in the actual site conditions and certain limitations present in the FE model.

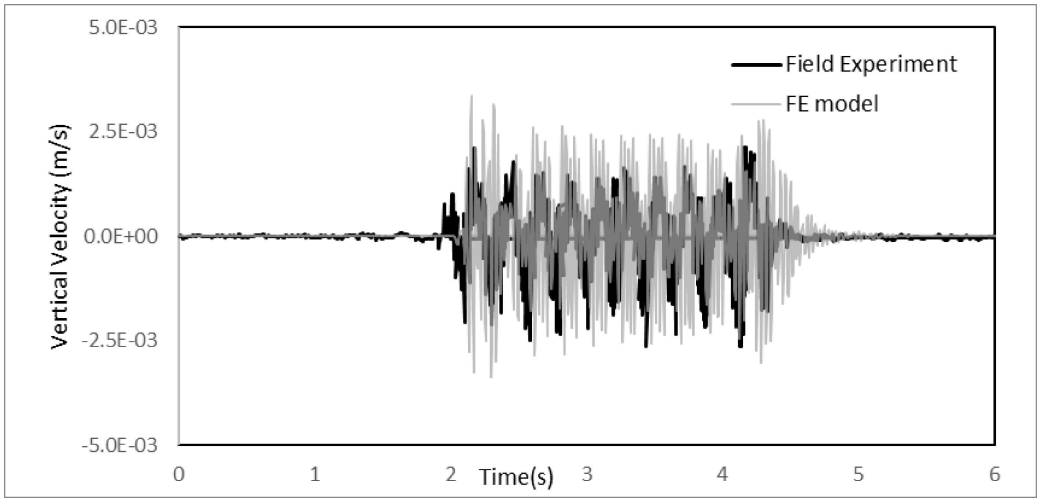

Figure 4.13: Comparison of Vertical PPV – time history variation at 6m

Figure 4.14 shows the variation of Vertical PPV at 8m from the railway track. Average Vertical PPV at 8m distance is closer to 1.8×10^{-3} m/s in both field experiment as well as FE simulation. Around 50% reduction in the Vertical PPV is observed at 8m distance compared to the intensity at 4m. Even though the distance between data set 2 and data set 3 is 4m, the PPV has reduced by a considerable amount of 0.002 m/s on average.

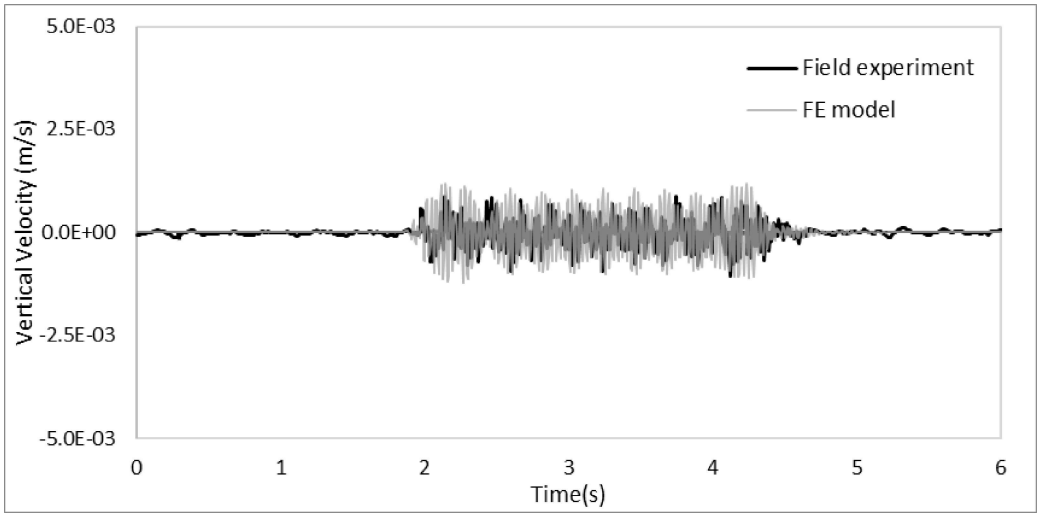

Figure 4.14: Comparison of Vertical PPV – time history variation at 8m

The vibration intensity at 12 m distance is shown in Figure 4.15. The average intensity lies around 0.8×10^{-3}m/s for both cases. Even though the FE simulation result shows a slight positive safe margin than field experiment result, it can be considered favorable.

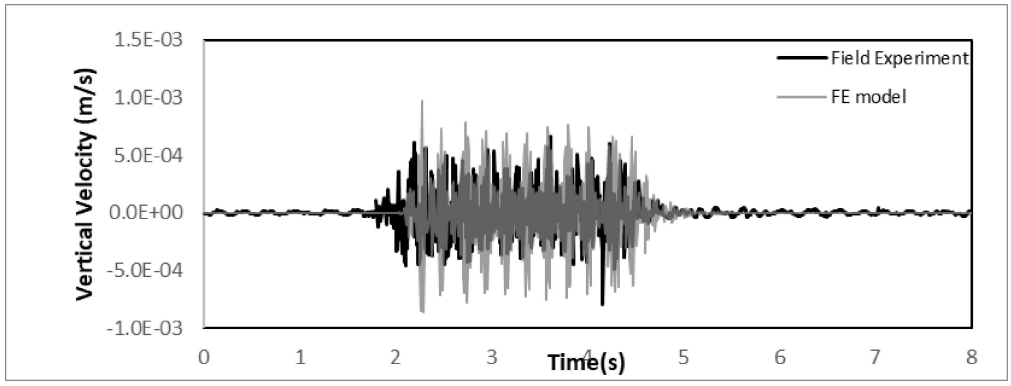

Figure 4.15: Comparison of Vertical PPV – time history variation at 12m

Table 4-4 and Figure 4.16 present a summary of the deviation of vertical PPV for all the aforementioned data sets. The maximum deviation observed is 15.63% at 6m, which falls within the acceptable range (considering 20% as the margin). This

finding demonstrates that the model results are reliable and provide a close prediction of vibration intensity, closely aligning with the actual data. Therefore, the developed FE model can be utilized to conduct a parametric study, simulating the response under varying train loads, soil properties, track properties, and moving speeds.

Table 4-4: Variation between FE simulation results and literature data

Distance from railway track	Literature data ($\times 10^{-3}$m/s)	FE simulation results ($\times 10^{-3}$m/s)	Deviation ($\times 10^{-3}$m/s)	Deviation as percentage
4 m	3.487	3.7138	0.2268	6.11%
6 m	2.656	3.148	0.492	15.63%
8 m	1.0904	1.1016	0.0112	1.02%
12 m	0.795	0.8642	0.0692	8.01%

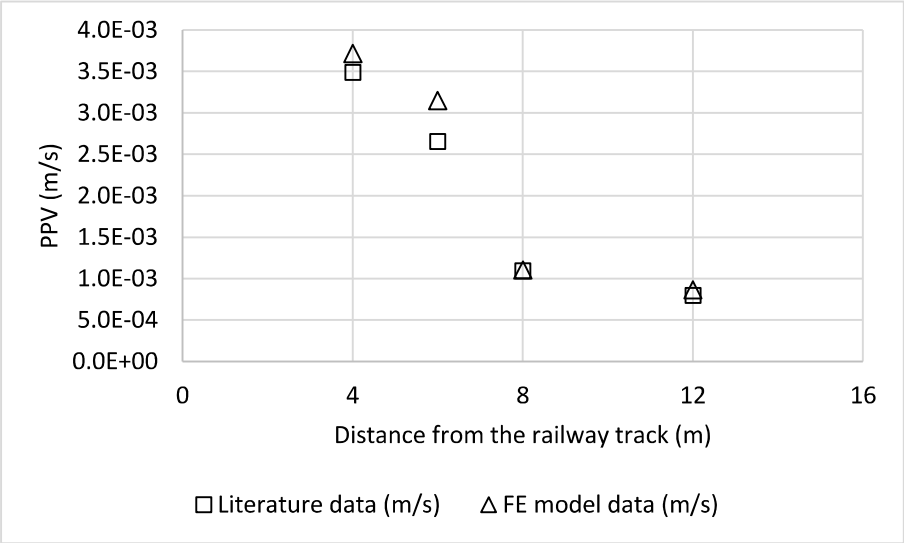

Figure 4.16 : Deviation of FE results with literature data

4.6 Parametric analysis using the FE prediction model.

After the successful validation, the FE prediction model is used for parametric analysis. The influence of parameters such as subgrade strength and speed are

assessed to identify the level of impact of the induced vibration. Table 4-5 shows the soil types and their material properties used in the FE analysis.

Table 4-5: Material properties of different soil types

Soil type	Elastic modulus (MPa)	Dry density (kgm^3)	Void ratio	Poisson ratio	Porosity	Friction angle (°)	Cu	Damping (%)	Shear strain (%)
Soft clay	20	1340	1.04	0.51	0.35	18	12	3.5	0.5-1.5
Hard clay	60	1840	0.89	0.47	0.29	20	50	4	0.5-1.5
Dense sand	80	1570	0.54	0.35	0.3	34	-	6	0.5-1.5
Medium sand and gravel	120	1740	0.67	0.40	0.31	30	-	7.5	0.5-1.5

Source: (Ishibashi & Zhang, 1993; Kokusho Takeji & Yoshida Yasuo, 1997; Kumar et al., 2017; Kyambadde & Stone, 2012; Mog & Anbazhagan, 2022; Obrzud & Truty, 2018; Shao et al., 2012)

Each component or structure of the FE model was meshed into appropriate mesh sizes according to the wave propagating velocity to have high accurate results. Hence, the selection of proper node at a particular distance is difficult in 3D analysis unlike 2D analysis. Therefore, the result for a particular analysis is obtained at various nodes to find the most detrimental result.

4.6.1 Analysis of the influence of soil type on the vibration intensity

Four different soil types; soft clay, hard clay, dense sand and medium sand and gravel were treated in this study. The material properties of the soil samples used in this study is presented in Table 4-5 under Chapter 4.6 Parametric analysis using the FE prediction model.

In this study, the dynamic load of the Thalys High-Speed Train (HST) traveling at a speed of 45 m/s was simulated. Figure 4.17 illustrates the variation of Vertical PPV with time at a distance of 3 m for four different soil types namely soft clay, hard clay, dense sand and medium sand and gravel. A drastic variation of vibration intensity is observed in the prediction result having the highest intensity of induced vibration for the soft clay and lowest intensity for the medium sand and gravel. The substantial variation in the subgrade strength and elastic modulus of the soil type is believed to be the primary cause for the differences observed in the results. However, detailed analysis was carried out to identify the influence of speed together with the soil properties. The soft clay, which has the lowest elastic modulus (20MPa), generates the highest vertical PPV of 4.2 mm/s, while the medium sand and gravel soil, with the highest elastic modulus (120GPa), produces the lowest vertical PPV. Since the speed remains constant throughout the simulations, the wave pattern along the x direction remains almost the same for all scenarios.

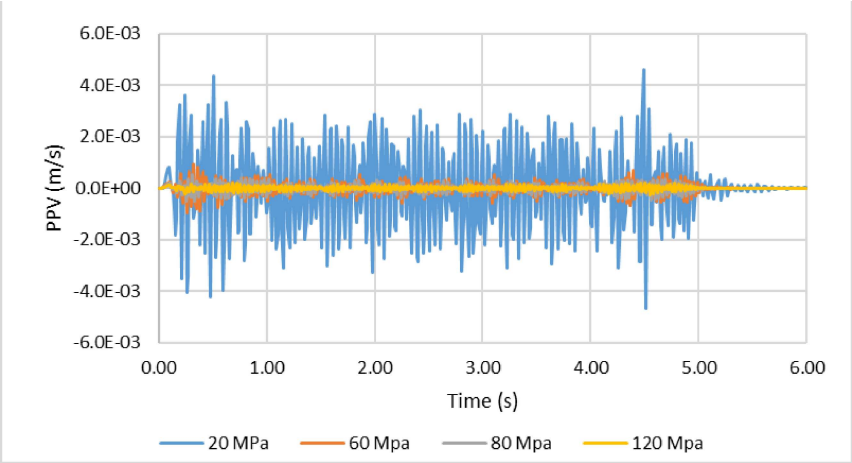

Figure 4.17: Variation of vertical PPV with time for varying subgrade strength

The simulation results presented in Figure 4.17 are summarized in the envelope shown in Figure 4.18. This plot illustrates the maximum, minimum, and average values of the vertical PPV for the train traveling at 45 m/s on four different soil types (soft clay, hard clay, dense sand, and medium sand and gravel). As the subgrade strength increases, a conical behaviour is observed, resulting in a narrowing down of the PPV to a negligible value. This indicates that a higher elastic modulus leads to reduced vibration intensity. However, a slight increase in the vibration was observed at a specific elastic modulus of the subgrade soil. The reason for this behaviour was particularly analysed by using controlled simulations.

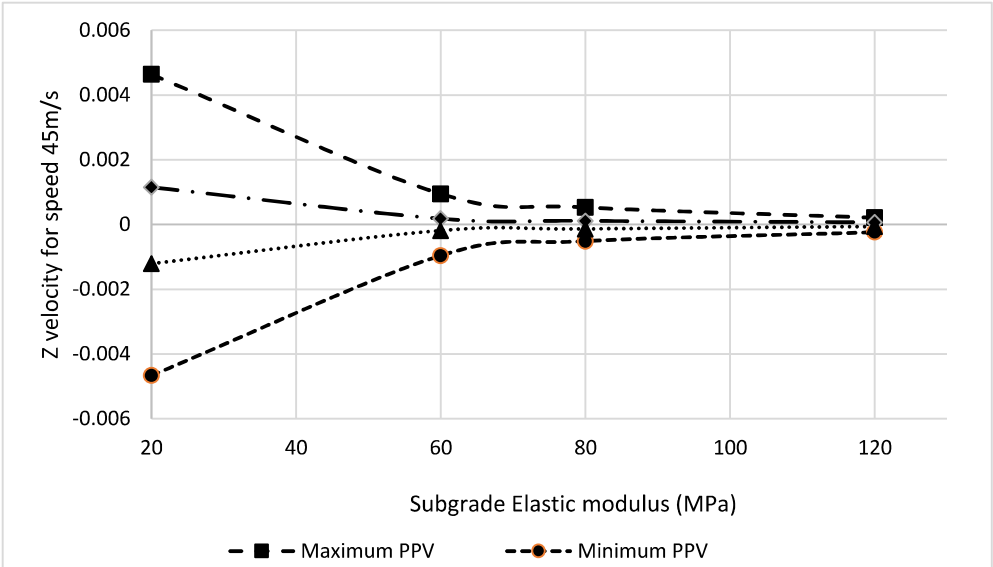

Figure 4.17: Variation of vertical PPV with the elastic modulus of the selected soil types for a train travelling at 45m/s

4.6.2 Analysis of the influence of speed on vibration intensity

This study was carried out for Thalys HST travelling on dense sand having an elastic modulus 80MPa. The effect of increasing train speed on vibration intensity (vertical PPV) was studied. The train speeds from 10 m/s to 150 m/s were analysed in this study. Practically, the Sri Lankan local train speed is limited from 10 m/s to 20 m/s. However, in most of the developed countries, the high-speed trains are operating at the speed of 60 m/s. A higher speed range was used in the analysis to predict the behaviour of the influence of speed on vibration. The results of this study are presented in the Figure 4.19. The degree of vibration increased with the speed of the

train gradually and a bell-shaped curve is occurred at a specific speed which is neither maximum speed nor minimum. For dense sand with 80 MPa elastic modulus, the highest vibration occurs at a speed of 85 m/s. This paved way for the study of critical velocity and resonance effects of ground borne vibration.

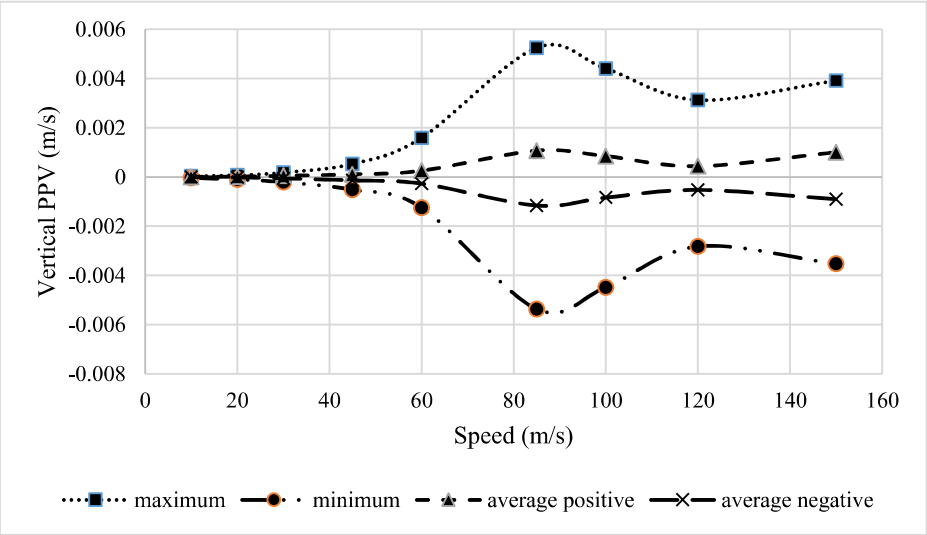

Figure 4.18: Variation of vertical PPV with speed for Dense sand with elastic modulus of 80MPa

The Figure 4.20 shows the variation of vertical PPV with speed for hard clay with elastic modulus of 60 MPa. Unlike the analysis of dense sand with elastic modulus 80MPa, the higher attenuation than the predicted is observed at two speeds namely 85 m/s, and 120 m/s. This unexpected result enforced even though the vibration intensity increases with speed, there may be some other factors influencing the intensity of vibration. This specific observation was an unexpected outcome of the study.

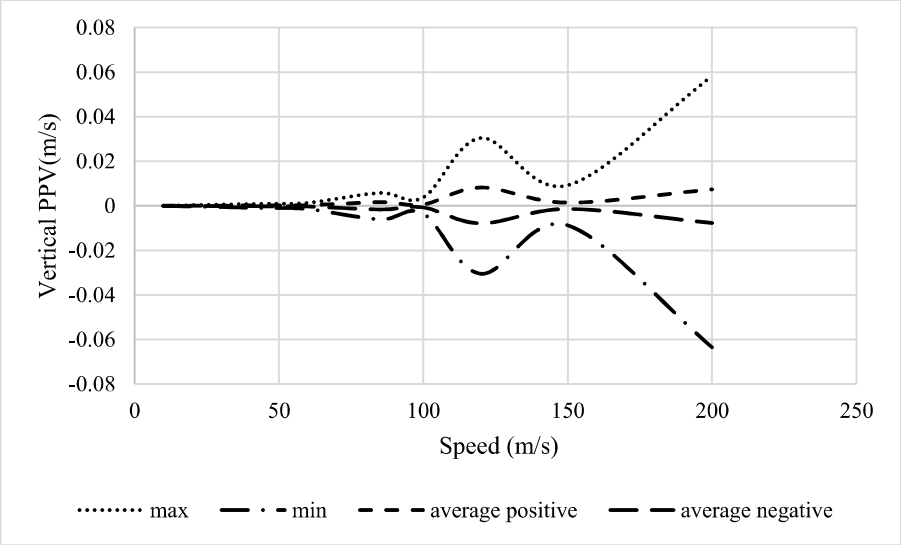

Figure 4.19: Variation of vertical PPV with speed for hard clay with elastic modulus of 60MPa

The analysis results were converted from time domain to frequency domain using Fast Fourier Transformation (FFT) for comprehensive analysis. The FFT of the simulations with speeds at 85m/s, 120 m/s and 150 m/s for 60 MPa subgrade strength are presented in the Figures 4.21-4.23 respectively.

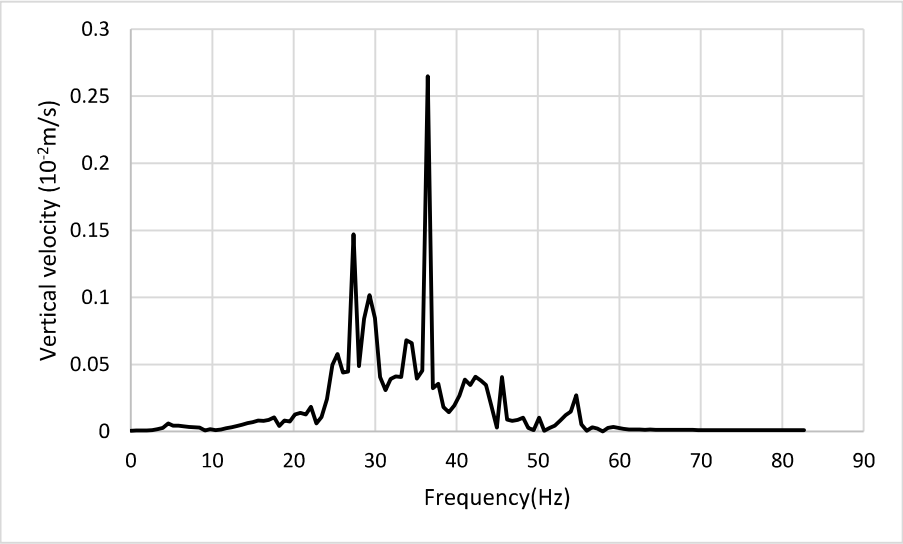

Figure 4.20: Variation of vertical velocity with frequency for the train travelling at speed 85m/s on hard clay

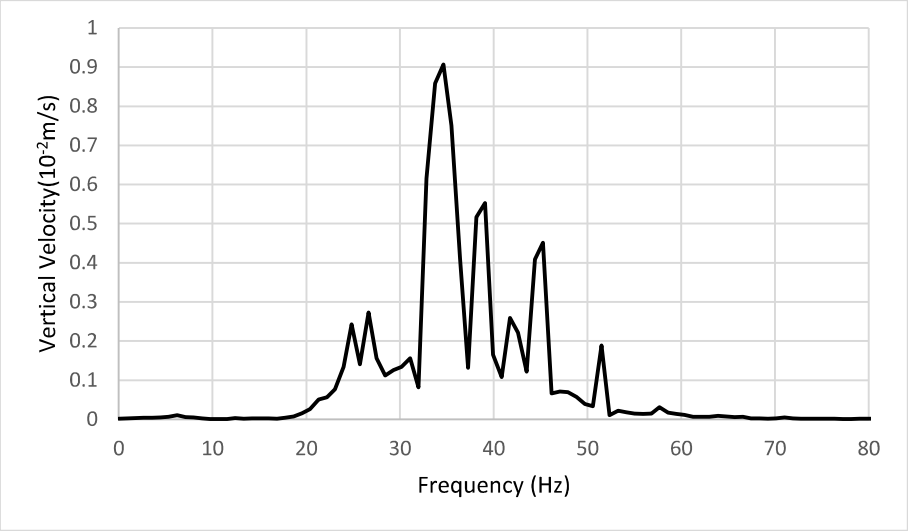

Figure 4.21: Variation of vertical velocity with frequency for the train traveling at 120 m/s on hard clay

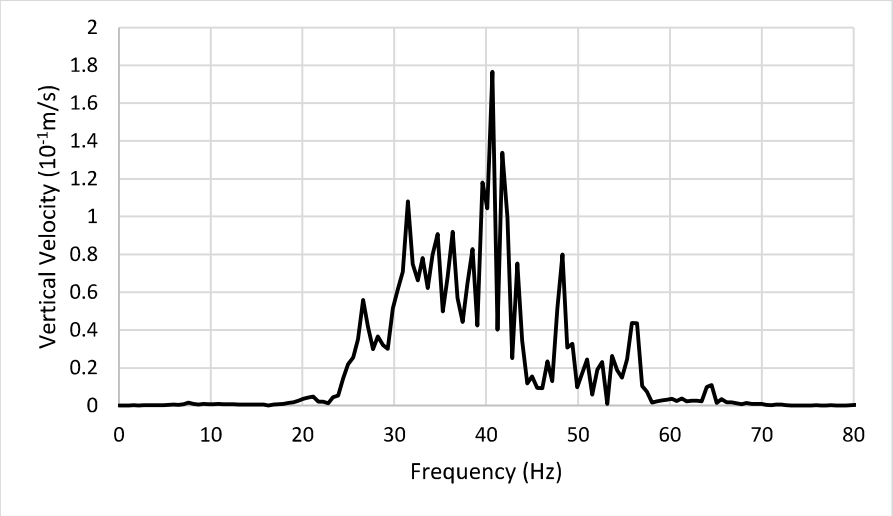

Figure 4.22: Variation of vertical velocity with frequency for the train traveling at 150 m/s on hard clay

From Figures 4.21-4.23, it is evident that the highest intensity of vibration occurs at frequencies of approximately 36.5Hz, 34.6Hz, and 40.7Hz for train speeds of 85 m/s, 120 m/s, and 150 m/s, respectively. When a vibrating body oscillates at a specific frequency and encounters another body with the same natural frequency, resonance occurs, resulting in an amplified resultant force. In Figures 4.21 and 4.22, higher

amplitudes of PPV are observed for frequencies closer to 36Hz. This phenomenon suggests the presence of resonance effects. Therefore, it can be deduced that the natural frequency of the soil structure is approximately 36Hz, which explains the higher amplification of Vertical PPV at that frequency.

Furthermore, similar analysis on speed variation was carried out for soft clay and medium sand and gravel and the results are shown in the Figures 4.24 and 4.25 respectively.

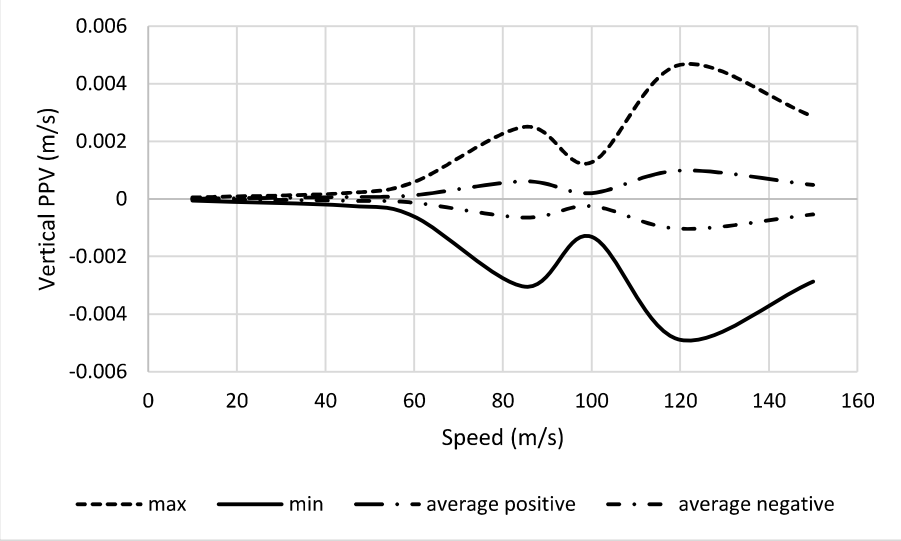

Figure 4.23: Variation of vertical PPV with speed for medium sand and gravel having E=120GPa

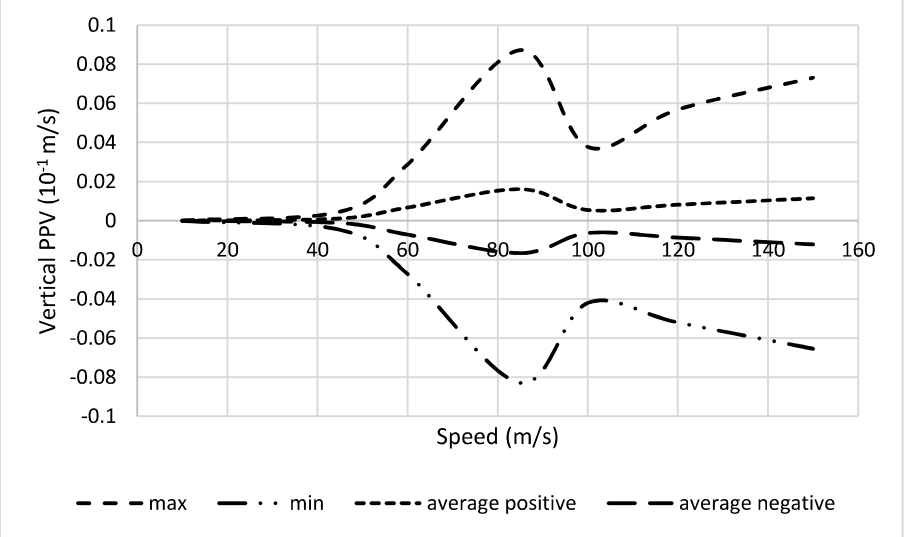

Figure 4.24: Variation of Vertical PPV with speed for soft clay soil having E= 20 MPa

The Figures 4.25-4.27 show the frequency history analysis of the vertical velocity for the soft clay, dense sand and the medium sand and gravel soil types. The results ensure that the different soil conditions posses different resonance frequency depending on the material properties of the subgrade. From the results, the resonance frequency for the train-track-soil system of the Thalys train traveling at the speed of 85 m/s on soft clay is around 28 Hz, dense sand is around 38 and the medium gravel and sand is around 29 Hz. The observed resonance frequencies are unpredictable and therefore the use of the prediction model is necessary.

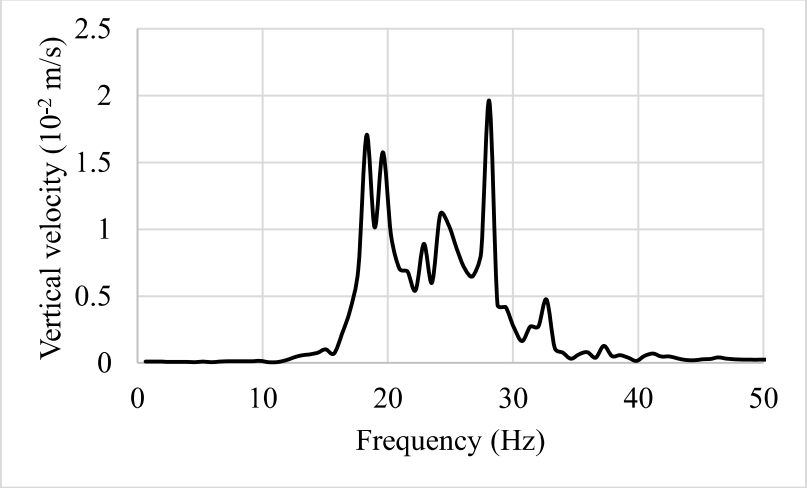

Figure 4.25: Variation of vertical velocity with frequency for the train traveling at 85 m/s on soft clay (E=20MPa)

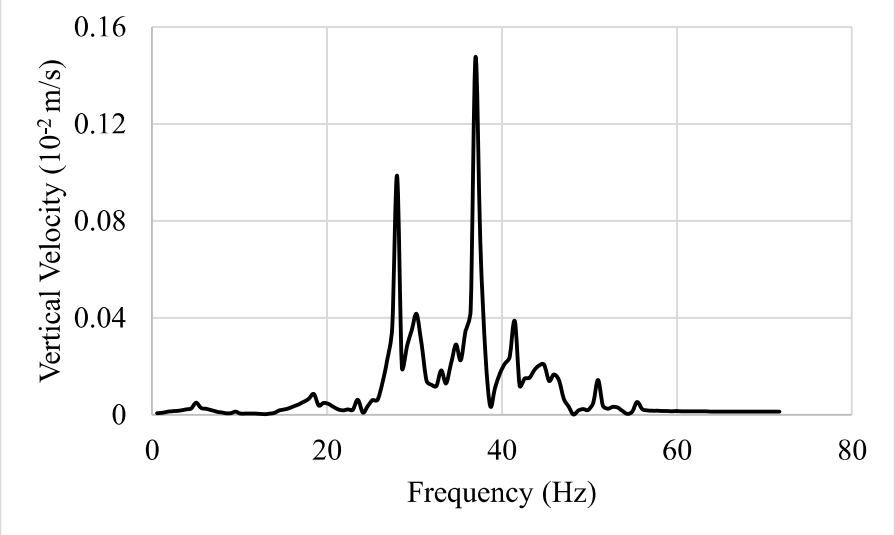

Figure 4.26: Variation of vertical velocity with frequency for the train traveling at 85 m/s on dense sand (E=80MPa)

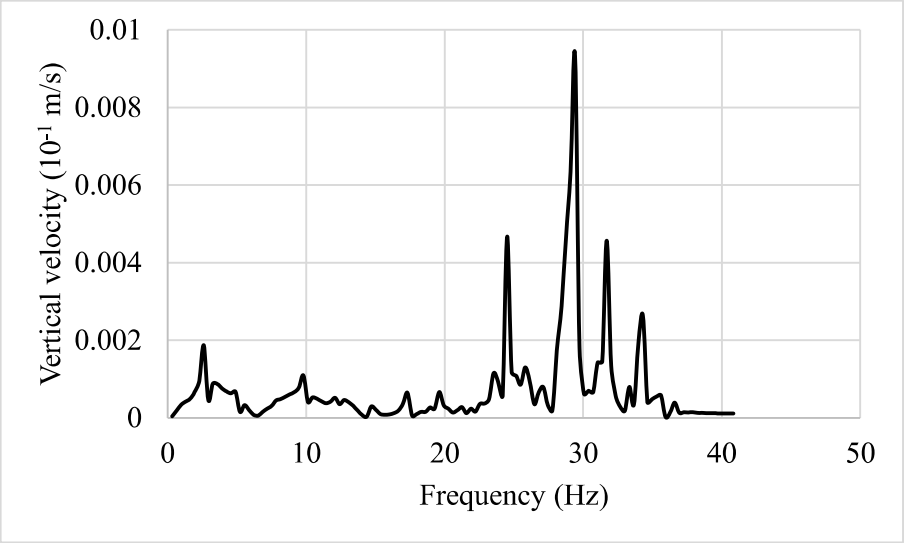

Figure 4.27: Variation of vertical velocity with frequency for the train traveling at 85 m/s on medium gravel and sand (E=120MPa)

4.7 Summary

This chapter presented the results obtained from the experimental study, validation of the FE model and the parametric study conducted using the FE model. The experimental results include soil investigation results, vibration intensity measured by the device and the variation of vertical PPV with the train speed. Next, the results obtained from numerical simulation were presented, and validated using the literature data and field experimental data. Finally, the results of the parametric study carried out to investigate the effects of soil type and train speed on the train-induced ground vibration and the identification of the resonance frequency and critical velocity were discussed in this chapter.

5. CONCLUSION AND RECOMMENDATION

5.1 Conclusion

This study aims to assess the intensity of train-induced ground vibrations through experimental analysis and a Finite Element (FE) prediction model. In this study, a vibration sensing device called "VIBSEN" was developed to measure ground vibrations. Vibration data were recorded at 3 m intervals (3 m, 6 m, 9 m, and 12 m) from the centreline of the railway track. The recorded data from VIBSEN were processed using MATLAB software, and the analysis results were then converted from the time domain to the frequency domain using Fast Fourier Transformation (FFT). The accuracy of the developed device was confirmed through gravity calibration and comparison with a vibrometer data.

Based on the experimental study conducted at the selected site between Koralawella and Moratuwa Railway Stations, it can be concluded that the minimum safe distance is approximately 10m from the centreline of the track when two trains cross simultaneously. When considering the passage of a single train, the minimum safe distance is approximately 6m. It is important to note that these recommendations are specific to the soil profile at the experimental site, and the minimum safe distances may vary depending on the subgrade soil type and its specific parameters. However, the developed VIBSEN device can be used for similar experimental investigations when required. The data obtained from a prolonged experimental study proposed in this research can be used to derive the safe distance for different types of buildings based on standard guidelines. This helps reduce the risk, structural failures, and hazards caused by prolonged exposure to vibrations.

The FE prediction model was developed using MIDAS GTS NX FE software to predict ground vibrations under a moving train load. The model was first validated using experimental results obtained from the present study for a Sri Lankan express train 8060. Subsequently, the model was used to simulate the passage of a Thalys High-Speed Train (HST) traveling at a speed of 314 km/h and compared with experimental results available in the literature (Degrande & Schillemans, 2001). These comparisons confirmed the applicability of the developed FE model in

predicting train-induced ground vibrations. After successful validation, parametric analysis was conducted to investigate the effects of soil type and train speed on train-induced ground vibrations, including the identification of resonance frequencies and critical velocities.

The findings of the parametric study can be summarized as follows: The effects of different soil types on vibration intensity were examined by modelling the dynamic load of the Thalys HST traveling at a speed of 45 m/s. Four different soil types, namely soft clay, hard clay, dense sand, and medium sand and gravel, with elastic moduli of 20, 60, 80, and 120 MPa, respectively, were considered. It was evident that the intensity of vibration significantly varies depending on the soil type, with lower intensities observed for soils with higher elastic moduli and increased intensities observed as the elastic modulus decreases.

Additionally, it was observed that while vibration intensity generally increases with increasing train speed, at certain speed levels, there is a sudden increase in intensity. This is believed to be due to the resonance effect of the soil and train-track system, with the corresponding velocity considered as the critical velocity of the system. For a specific soil type, there may be multiple critical velocities. The analysis of vibration intensity vs. frequency also showed that the resonance frequency can vary depending on the elastic modulus of the subgrade soil.

5.2 Recommendation for future works

This research can be further extended by conducting research on following areas:

- **Developing realistic models using digital twinning** : Modelling the existing system and incorporating with the actual data set to create a digital twin of the system will improve the real time monitoring of the railway system and associated structures.

- **Extensive parametric analysis using Artificial Neural Network**: Apart from the known factors influencing the vibration intensity, using Artificial

Neural Network to analyze the big data will efficiently produce algorithms to predict railway induced vibration.

- **Developing mitigation measures and efficiency:** The measures to identify high intense location and developing suitable mitigation methods such as trenches, and floating slab system could be studied further and an optimum material property can be identified.

- **Consideration of Train-Track-Structure Interaction**: Enhance the prediction models by incorporating the dynamic interaction between trains, tracks, and surrounding structures. This will help to capture more realistic vibration responses and improve the accuracy of predictions in complex railway systems.

- **Consideration of Environmental and Human Factors**: Extend the research to investigate the effects of vibrations on the surrounding environment, nearby communities, and human comfort. This holistic approach will contribute to the understanding of broader implications and facilitate the implementation of appropriate mitigation measures.

REFERENCES

British Standards Institution. (1993). *Evaluation and measurement for vibration in buildings-Part 2: Guide to damage levels from ground borne vibration* (BS 7385-2-1993).

Al Suhairy, S. (2000). *Prediction of Ground Vibration from Railways* [Master of Science thesis, Department of Applied Acoustics, Chalmers University of Technology]. http://urn.kb.se/resolve?urn=urn:nbn:se:ri:diva-4509

Auersch, L. (2010). Building Response due to Ground Vibration — Simple Prediction Model Based on Experience with Detailed Models and Measurements. *International Journal of Acoustics and Vibrations,* 15(3), 101-112. https://doi.org/10.20855/ijav.2010.15.3262

Bogacz, R., & Bajer, C. (2015, March). *Vibration of the train / track system with two types of sleepers* [Paper presentation]. Conference on Vibrations in Physical Systems, 2015. https://www.researchgate.net/publication/268181278_Vibration_of_the_traintrack_system_with_two_types_of_sleepers#fullTextFileContent

British Standards Institution. (2008). *Guide to evaluation of human exposure to vibration in buildings Part 1: Vibration sources other than blasting* (BS 6472-1-2008).

Connolly, D., Giannopoulos, A., & Forde, M. C. (2013). Numerical modelling of ground borne vibrations from high speed rail lines on embankments. *Soil Dynamics and Earthquake Engineering*, *46*, 13–19. https://doi.org/10.1016/j.soildyn.2012.12.003

Connolly, D. P., Kouroussis, G., Woodward, P. K., Costa, P. A., Verlinden, O., & Forde, M. C. (2014). Field testing and analysis of high speed rail vibrations. *Soil Dynamics and Earthquake Engineering*, *67*, 102–118. https://doi.org/10.1016/j.soildyn.2014.08.013

Correia, N., Colaço, A., Costa, P. A., & Calçada, R. (2016). Experimental analysis of

track-ground vibrations on a stretch of the Portuguese railway network. *Soil Dynamics and Earthquake Engineering*, *90*, 358–380. https://doi.org/10.1016/j.soildyn.2016.09.003

Degrande, G., & Schillemans, L. (2001). Free field vibrations during the passage of a thalys high-speed train at variable speed. *Journal of Sound and Vibration*, *247*(1), 131–144. https://doi.org/10.1006/jsvi.2001.3718

Deraemaeker, A., Reynders, E., De Roeck, G., & Kullaa, J. (2008). Vibration-based structural health monitoring using output-only measurements under changing environment. *Mechanical Systems and Signal Processing*, *22*(1), 34–56. https://doi.org/10.1016/j.ymssp.2007.07.004

Dijckmans, A., Coulier, P., Jiang, J., Toward, M. G. R., Thompson, D. J., & Degrande, G. (2015). Mitigation of railway induced ground vibration by heavy masses next to the track. *Soil Dynamics and Earthquake Engineering*, *75*, 158–170. https://doi.org/10.1016/j.soildyn.2015.04.003

German Institute of Standardization. (1999). *Structural vibration Part 2: Hunam exposure to vibration in buildings* (DIN-4150-2-1999).

Do Rêgo Silva, J. J. (1994). *Acoustic and elastic wave scattering using boundary elements: Volume 18 of Topics in Engineering*. Computational Mechanics Publications. https://books.google.lk/books?id=ZMIyngEACAAJ

François, S., Galvín, P., Schevenels, M., Lombaert, G., & Degrande, G. (2012). A 2.5D Coupled FE-BE Methodology for the Prediction of Railway Induced Vibrations. *Noise and Vibration Mitigation for Rail Transportation Systems*, (PP 367–374). Notes on Numerical Fluid Mechanics and Multidisciplinary Design, vol 118. Springer, Tokyo. https://doi.org/10.1007/978-4-431-53927-8_43 .

Brinkgreve, RBJ., & Galavi, V. (2014). Finite element modelling of geotechnical structures subjected to moving loads. In MA. Hicks, RBJ. Brinkgreve, & A. Rohe (Eds.), *Proceedings of the 8th European conference on numerical*

methods in geotechnical engineering (pp. 235-240). Taylor and Francis. https://doi.org/10.1201/b17017-44.

Grassie, S. L., Gregory, R. W., Harrison, D., & Johnson, K. L. (1982). The Dynamic Response of Railway Track to High Frequency Vertical Excitation. *Journal of Mechanical Engineering Science*, *2*(24), 77–90. https://doi.org/10.1243/jmes_jour_1982_024_016_02

Heckl, M., Hauck, G., & Wettschureck, R. (1996). Structure-borne sound and vibration from rail traffic. *Journal of Sound and Vibration*, *193*(1), 175–184. https://doi.org/10.1006/jsvi.1996.0257

Hu, J., Luo, Y., Ke, Z., Liu, P., & Xu, J. (2018). Experimental study on ground vibration attenuation induced by heavy freight wagons on a railway viaduct. *Journal of Low Frequency Noise, Vibration and Active Control*, *37*(4), 881–895. https://doi.org/10.1177/1461348418765949

Indraratna, B., Nimbalkar, S., & Rujikiatkamjorn, C. (2012). Track Stabilisation with Geosynthetics and Geodrains, and Performance Verification through Field Monitoring and Numerical Modelling. *International Journal of Railway Technology*, *1*(1), 195–219. https://doi.org/10.4203/ijrt.1.1.9

Indraratna, Buddhima, & Nimbalkar, S. (2013). Stress-Strain Degradation Response of Railway Ballast Stabilized with Geosynthetics. *Journal of Geotechnical and Geoenvironmental Engineering*, *139*(5), 684–700. https://doi.org/10.1061/(asce)gt.1943-5606.0000758

Ishibashi, I., & Zhang, X. (1993). Unified Dynamic Shear Moduli and Damping Ratios of Sand and Clay. *Soils and Foundations*, *33*(1), 182–191. https://doi.org/10.3208/sandf1972.33.182

British standards institution. (2005). *Mechanical vibration — Ground-borne noise and vibration arising from rail systems — Part 1 : General guidance* (ISO 14837-1-2005).

Iwnicki, S. (Ed.) (2006). *Handbook of Railway Vehicle Dynamics.* (1st ed.) CRC Press. https://doi.org/10.1201/9781420004892

Jayawardana, P., Achuhan, R., Silva, G. H. M. J. S. De, & Thambiratnam, D. P. (2018). Use of in- filled trenches to screen ground vibration due to impact pile driving : experimental and numerical study. *Heliyon, 4(8), e00726. https://doi.org/10.1016/j.heliyon.2018.e00726*

Jik Lee, P., & Griffin, M. J. (2013). Combined effect of noise and vibration produced by high-speed trains on annoyance in buildings. *The Journal of the Acoustical Society of America*, *133*(4), 2126–2135. https://doi.org/10.1121/1.4793271

Khordehbinan, M. W. (2009). *Sensitive analysis of granular layers of rail support system in the ballasted railway tracks of Iran*.[Master of Science dissertation, University of Tehran].

Kokusho Takeji, & Yoshida Yasuo. (1997). SPT-N value and S-wave velocity for gravelly soils with different grain size distribution. *Soils and Foundations*, 37(4), 105–113. https://doi.org/10.3208/sandf.37.4_105

Kouroussis, G., Connolly, D. P., & Verlinden, O. (2014). Railway-induced ground vibrations – a review of vehicle effects. *International Journal of Rail Transportation*, *2*(2), 69–110. https://doi.org/10.1080/23248378.2014.897791

Kouroussis, Georges, Connolly, D. P., Olivier, B., Laghrouche, O., & Costa, P. A. (2016). Railway cuttings and embankments: Experimental and numerical studies of ground vibration. *Science of the Total Environment*, *557–558*, 110–122. https://doi.org/10.1016/j.scitotenv.2016.03.016

Kouroussis, G., Verlinden, O., Connolly, D., & Forde, M. (2013). An experimental study of embankment conditions on high-speed railway ground vibrations. *In 20th International Congress on Sound and Vibration 2013*, ICSV 2013, 4(1), (pp 3034-3041). https://www.scopus.com/record/display.uri?eid=2-s2.0-84897090453&origin=inward&txGid=c7db52a7fa86c3c850c002795817ca51

Kouroussis, Georges, Verlinden, O., & Conti, C. (2011). Finite-Dynamic Model for Infinite Media: Corrected Solution of Viscous Boundary Efficiency. *Journal of Engineering Mechanics*, *137*(7), 509–511. https://doi.org/10.1061/(ASCE)EM.1943-7889.0000250

Kouroussis, Georges, Verlinden, O., & Conti, C. (2012). Efficiency of resilient wheels on the alleviation of railway ground vibrations. *Proceedings of the Institution of Mechanical Engineers, Part F: Journal of Rail and Rapid Transit*, *226*(4), 381–396. https://doi.org/10.1177/0954409711429210

Krylov, V. V. (1994). On the theory of railway-induced ground vibrations. *Journal of Physics,* 4(1), 769-772. https://doi.org/10.1051/jp4:19945167

Kulkarni, M. P., Patel, A., & Singh, D. N. (2010). Application of shear wave velocity for characterizing clays from coastal regions. *KSCE Journal of Civil Engineering*, *14*(3), 307–321. https://doi.org/10.1007/s12205-010-0307-1

Kumar, S. S., Krishna, A. M., & Dey, A. (2017). Evaluation of dynamic properties of sandy soil at high cyclic strains. *Soil Dynamics and Earthquake Engineering*, *99*(May 2016), 157–167. https://doi.org/10.1016/j.soildyn.2017.05.016

Kyambadde, B. S., & Stone, K. J. L. (2012). Index and strength properties of clay-gravel mixtures. *Proceedings of the Institution of Civil Engineers: Geotechnical Engineering*, *165*(1), 13–21. https://doi.org/10.1680/geng.2012.165.1.13

Li, Q., Luo, Y., & Liu, Y. (2016). Experimental research on identification of ground-borne noise from subway lines based on partial coherence analysis. *Procedia Engineering*, *144*, 1150–1157. https://doi.org/10.1016/j.proeng.2016.05.085

Lombaert, G. Ã., Degrande, G., Kogut, J., & Franc, S. (2006). The experimental validation of a numerical model for the prediction of railway induced vibrations. *Journal of Sound and Vibration, 297*, 512–535. https://doi.org/10.1016/j.jsv.2006.03.048

Longinow, A., & Mohammadi, J. (2023). Effects of Vibrations on Structures :

Overview and Case Studies. *Practice Periodical on Structural Design and Construction*, 27(4), 1–8. https://doi.org/10.1061/(ASCE)SC.1943-5576.0000730

Lopes, P., Ruiz, J. F., Alves Costa, P., Medina Rodríguez, L., & Cardoso, A. S. (2016). Vibrations inside buildings due to subway railway traffic. Experimental validation of a comprehensive prediction model. *Science of the Total Environment*, *568*, 1333–1343. https://doi.org/10.1016/j.scitotenv.2015.11.016

Madshus, C., & Kaynia, A. M. (2000). High-speed railway lines on soft ground: dynamic behaviour at critical train speed. *Journal of Sound and Vibration*, *231*(3), 689–701. https://doi.org/10.1006/jsvi.1999.2647

Magalhaes, F., Cunha, A., & Caetano, E. (2012). Vibration based structural health monitoring of an arch bridge : From automated OMA to damage detection. *Mechanical Systems and Signal Processing, 28*, 212–228. https://doi.org/10.1016/j.ymssp.2011.06.011

Maldonado, M., Chiello, O., & Houédec, D. (2008) Propagation of Vibrations Due to a Tramway Line. *Noise and Vibration Mitigation for Rail Transportation Systems* (pp. 158–164). Springer Berlin Heidelberg. https://doi.org/10.1007/978-3-540-74893-9_22.

Mog, K., & Anbazhagan, P. (2022). Evaluation of the damping ratio of soils in a resonant column using different methods. *Soils and Foundations*, *62*(1), 101091. https://doi.org/10.1016/j.sandf.2021.101091

Derrick, N., & Srivastava, A. K. (2020). Effect of Mesh Size on Soil-Structure Interaction in Finite Element Analysis. *International Journal of Engineering Research And*, *9*(6), 802–807. https://doi.org/10.17577/ijertv9is060655

Obrzud, R. F., & Truty, A. (2018). *The hardening soil model - A practical guide book. 05*. http://www.zsoil.com/zsoil_manual_2018/Rep-HS-model.pdf

Ögren, M., Gidlöf-Gunnarsson, A., Smith, M., Gustavsson, S., & Waye, K. P.

(2017). Comparison of annoyance from railway noise and railway vibration. *International Journal of Environmental Research and Public Health*, *14*(7). https://doi.org/10.3390/ijerph14070805

Okumura, Y., & Kuno, K. (1991). Statistical analysis of field data of railway noise and vibration collected in an urban area. *Applied Acoustics*, *33*(4), 263–280. https://doi.org/10.1016/0003-682X(91)90017-9

Pap, Z. B., & Kollár, L. P. (2018). Effect of Resonance in Soil-Structure Interaction for Finite Soil Layers. *Periodica Polytechnica Civil Engineering*, 62(3), 676–684, 2018. https://doi.org/10.3311/PPci.11960

Prakoso, P. B. (2012). The Basic Concepts of ModellingRailway Track Systems usingConventional and Finite Element Methods. *Info Teknik*, *13*(1), 57–65.

Shaltout, R. E., Ulianov, C., & Chen, H. M. (2015). Coupled numerical modelling of railway track substructure with vehicle-track interaction. Keuis, J., Tsompanakis, Y., & Topping, B. H. V (Eds). *Proceedings of the Fifteenth International Conference on Civil, Structural and Environmental Engineering (2015)*, 108, Civil-Comp Proceedings.

Romero, A., Galvin, P., & Dominguez, J. (2012). A time domain analysis of train induced vibrations. *Earthquakes and Structures*, 3(3_4), 297–313. https://doi.org/10.12989/eas.2012.3.3_4.297

Sayeed, M. A., & Shahin, M. A. (2016). Three-dimensional numerical modelling of ballasted railway track foundations for high-speed trains with special reference to critical speed. *Transportation Geotechnics*, *6*, 55–65. https://doi.org/10.1016/j.trgeo.2016.01.003

Shao, Y., Shi, B., Liu, C., & Gao, L. (2012). Experimental study on temperature effect on engineering properties of clayey soils. *Advanced Materials Research*, *512–515*, 1905–1918. https://doi.org/10.4028/www.scientific.net/AMR.512-515.1905

Sheng, X., Jones, C. J. C., & Thompson, D. J. (2004). A theoretical study on the influence of the track on train-induced ground vibration. *Journal of Sound and Vibration.* 272(3-5), 909–936. https://doi.org/10.1016/S0022-460X(03)00781-8

International Organisation for Standardisation. (1997). *Mechanical vibration and shock – Evaluation of human exposure to whole-body vibration – part 1: General requirements* (ISO 2631-1-1997).

International Organisation for Standardisation. (2009). *Mechanical vibration - Evaluation of machine vibration by measurements on nonrotating parts - Part 7: Rotodynamic pumps for industrial applications, including measurements on rotating shafts* (BS ISO 10816-3-2009).

Svinkin, M. R., & Asce, M. (2014). Tolerable Limits of Construction Vibrations. *Practice Periodical on Structural Design and Construction*, 20(2), 1–7. doi:10.1061/(ASCE)SC.1943-5576.0000223.

ST Microelectronics. (2017). *LIS3DHH adapter board for a standard DIL 24 socket*. *June*, 1–4. https://www.st.com/resource/en/data_brief/steval-mki180v1.pdf

Thadsanamoorthy, P., & Damruwan, H. G. H. (2020). Intensity of Ground Vibration During the Passage of Trains : A Case Study. https://easychair.org/publications/preprint/3l9H

Vithrana, V. H. P., Silva, G. H. M. J. S. De., & Silva, G. S. Y. De. (2013). Risk associated with noise and vibration exposures and their effects on health of workers in construction sites. *Proceedings of the 4th International conference on Structural Engineering and Construction Management 2013*, 66–79.

Woldringh, R. F., & New, B. M. (1999). Embankment design for high speed trains on soft soils. *Geotechnical Engineering for Transportation Infrastructure. Proceedings of the 12th European Conference on Soil Mechanics and Geotechincal Engineering, Amsterdam, June 1999. Vol. 3.*, 1703–1712.

Xu, J., Yan, C., Zhao, X., Du, K., & Li, H. (2017). Monitoring of train-induced

vibrations on rock slopes. *International Journal of Distributed Sensor Networks.* 2017, 13(1). doi:10.1177/1550147716687557

Yang, W., Cui, G., Xu, Z., Yan, Q., He, C., & Zhang, Y. (2018). An experimental study of ground-borne vibration from shield tunnels. *Tunnelling and Underground Space Technology*, *71*(2017), 244–252. https://doi.org/10.1016/j.tust.2017.08.020

Zhu, S., Shi, X., Leung, R., Ng, S., Zhang, X., & Wang, Y. (2014). Impact of Construction-Induced Vibration on Vibration-Sensitive Medical Equipment: A Case Study. *Advances in Structural Engineering*, *17*, 907–920. https://doi.org/10.1260/1369-4332.17.6.907

APPENDICES

Appendix-A : Matlab code for signal processing

```
clc;
start = 1;
fid=readtable('C:\Users\User\Desktop\location1\Data2019-11-2118-22-8.txt');
time = fid.Time_s_;
x = fid.Z_m_s2_;
time = time(start:end);
x = x(start:end);

x = x - mean(x);
Fs  = 1/(time(2)-time(1));

figure(1)
plot(time,x)
ax = gca;
ax.YAxis.Exponent = 2;
xlabel('Time (s)');
ylabel('Accel(m/s2)');
title('Measurement');
grid on;

% Frequency spectrum
N = length(time);
freq1 = 0:Fs/length(x):Fs/2; %frequency array for FFT
xdft = fft(x); %Compute FFT
%ff = fftshift(xdft);
xdft = 1/length(x).*xdft; %Normalize
xdft(2:end-1) = 2*xdft(2:end-1);
```

```
figure(2)
plot(freq1,abs(xdft(1:floor(N/2)+1)))
xlabel('Frequency (Hz)');
ylabel('Accel(m/s2)');
title('FFT');
grid on;

% Lowpass filtering (filter out noise component greater than 2 hz)
Fpass = 49;
Fstop = 50;
Rp = 0.1;
Astop = 80;
LPF = dsp.LowpassFilter('SampleRate',Fs,...
                        'FilterType','FIR',...
                        'PassbandFrequency',Fpass,...
                        'StopbandFrequency',Fstop,...
                        'PassbandRipple',Rp,...
                        'StopbandAttenuation',Astop);

Output1 = step(LPF, x);


% Highpass filtering (filter out noise component greater than 2 hz)
Fpass = 45;
Fstop = 44;
Rp = 0.1;
Astop = 80;
HPF = dsp.HighpassFilter('SampleRate',Fs,...
                        'FilterType','FIR',...
                        'PassbandFrequency',Fpass,...
                        'StopbandFrequency',Fstop,...
                        'PassbandRipple',Rp,...
```

```
                    'StopbandAttenuation',Astop);

Output = step(HPF, Output1);
figure (3)
plot(time,Output);
title('Denoise')
xlabel('Time (s)');
ylabel('Accel(m/s2)');
grid on;

xdft = fft(Output); %Compute FFT
xdft = 1/length(x).*xdft; %Normalize
xdft(2:end-1) = 2*xdft(2:end-1);

figure(4)
plot(freq1,abs(xdft(1:floor(N/2)+1)))
xlabel('Frequency (Hz)');
ylabel('Accel(m/s2)');
title('FFT after lowpass filter');
grid on;

velocity = cumtrapz(time,Output);
figure(5)
plot(time,velocity);
title('velocity');
xlabel('Time(s)');
ylabel('Velocity(m/s)');

% Frequency spectrum
N = length(time);
freq1 = 0:Fs/length(x):Fs/2; %frequency array for FFT
xdft = fft(velocity); %Compute FFT
```

```
%ff = fftshift(xdft);
xdft = 1/length(x).*xdft; %Normalize
xdft(2:end-1) = 2*xdft(2:end-1);

figure(6)
plot(freq1,abs(xdft(1:floor(N/2)+1)))
xlabel('Frequency (Hz)');
ylabel('Velocity(m/s)');
title('FFT');
grid on;
```

Appendix B – Borehole report of the locations at the vicinity of field test

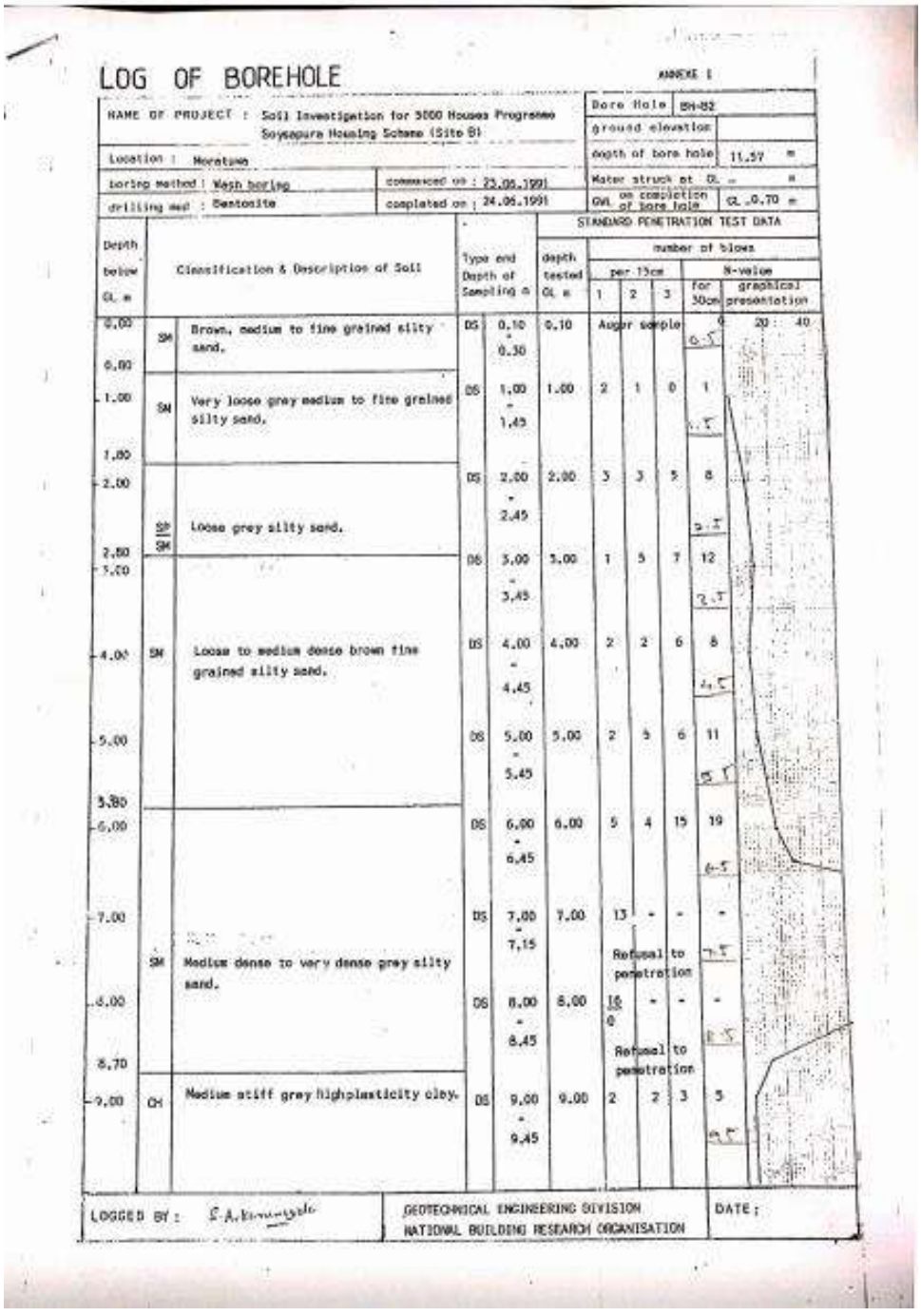

ANNEXE I

LOG OF BOREHOLE

NAME OF PROJECT : Soil Investigation for 5000 Houses Programme Soysapura Housing Scheme (Site B)

Location : Moratuwa

Boring method : Wash boring — commenced on : 23.06.1991

drilling mud : Bentonite — completed on : 24.06.1991

Bore Hole : BH-B2

ground elevation :

depth of bore hole : 11.57 m

Water struck at GL ... m

GWL on completion of bore hole : GL -0.70 m

Depth below GL m	Classification & Description of Soil	Type and Depth of Sampling m	depth tested GL m	STANDARD PENETRATION TEST DATA: number of blows per 15cm (1 / 2 / 3)	N-value for 30cm	N-value graphical presentation
0.00	SM Brown, medium to fine grained silty sand.	DS 0.10 - 0.30	0.10	Auger sample		0.5
1.00	SM Very loose grey medium to fine grained silty sand.	DS 1.00 - 1.45	1.00	2 / 1 / 0	1	1.5
2.00	SP/SM Loose grey silty sand.	DS 2.00 - 2.45	2.00	3 / 3 / 5	8	2.5
2.80						
3.00	SM Loose to medium dense brown fine grained silty sand.	DS 3.00 - 3.45	3.00	1 / 5 / 7	12	3.5
4.00		DS 4.00 - 4.45	4.00	2 / 2 / 6	8	4.5
5.00		DS 5.00 - 5.45	5.00	2 / 5 / 6	11	5.5
5.80						
6.00		DS 6.00 - 6.45	6.00	5 / 4 / 15	19	6.5
7.00	SM Medium dense to very dense grey silty sand.	DS 7.00 - 7.15	7.00	13 / - / -	- Refusal to penetration	7.5
8.00		DS 8.00 - 8.45	8.00	15/0 / - / -	- Refusal to penetration	8.5
8.70						
9.00	CH Medium stiff grey highplasticity clay.	DS 9.00 - 9.45	9.00	2 / 2 / 3	5	9.5

LOGGED BY : S.A.Kumarage — GEOTECHNICAL ENGINEERING DIVISION, NATIONAL BUILDING RESEARCH ORGANISATION — DATE :

LOG OF BOREHOLE

ANNEXE 1

NAME OF PROJECT : Soil Investigation for 5000 House Programme Soysapura Housing Scheme (Site B)		Bore Hole	BH-02 Contd.
		ground elevation	
Location : Moratuwa		depth of bore hole	11.57 m
boring method : Wash boring	commenced on : 23.06.1991	Water struck at GL -	m
drilling mud : Bentonite	completed on : 24.06.1991	GWL on completion of bore hole	GL -0.70 m

Depth below GL m	Classification & Description of Soil	Type and Depth of Sampling m	depth tested GL m	STANDARD PENETRATION TEST DATA: number of blows per 15cm 1	2	3	N-value for 30cm	N-value graphical presentation
10.00	Sample not recovered (Grey clay with little sand)	10.00 - 10.45	10.00	1	2	3	5	
11.00	Sample not recovered	11.00 - 11.45	11.00	1	2	3	5	
11.57	Borehole terminated at 11.57m depth	11.55 - 11.57	11.55	30/2	-	-	-	
12.00								
13.00								
14.00								

LOGGED BY : C.A. Ranasinghe	GEOTECHNICAL ENGINEERING DIVISION NATIONAL BUILDING RESEARCH ORGANISATION	DATE :

Appendix C: Intensity of vibration during railway passage from the experimental analysis

Train no	Track no	From-To	Time taken (s)	Speed (km/h)	PPV@3m (mm/s)	PPV@6m (mm/s)	PPV@7.2m (mm/s)	PPV@9m (mm/s)	PPV@10.2m (mm/s)	PPV@12m (mm/s)	PPV@13.2m (mm/s)	PPV@16.2m (mm/s)
1	1	G-M	2.84	82.38	22.12	15.28	N/A	10.12	N/A	5.21	N/A	N/A
2	1	G-M	3.40	68.74	19.46	13.3	N/A	7.27	N/A	3.82	N/A	N/A
3	1	G-M	5.28	44.32	11.2	7.61	N/A	4.22	N/A	1.03	N/A	N/A
4	1	G-M	4.79	48.85	12.4	8.75	N/A	4.61	N/A	1.06	N/A	N/A
5	2	M-G	5.06	46.25	N/A	N/A	2.81	N/A	0.52	N/A	N/A	N/A
6	2	M-G	4.36	53.66	N/A	N/A	6.48	N/A	2.6	N/A	N/A	N/A
7	2	M-G	4.82	48.55	N/A	N/A	7.21	N/A	2.17	N/A	1.76	1.3

8	1	G-M	4.27	54.80	15.29	8.17	N/A	6.47	N/A	2.05	N/A	N/A
9	2	G-M	3.53	66.29	N/A	N/A	9.94	N/A	4.29	N/A	2.65	N/A
10	1	G-M	3.18	73.58	17.24	12.45	N/A	8.18	N/A	6.1	N/A	N/A
11	1	G-M	3.86	60.62	15.67	10.02	N/A	6.35	N/A	2.43	N/A	N/A
12	1	G-M	3.85	60.78	15.47	11.97	N/A	7.02	N/A	2.63	N/A	N/A
13	2	M-G	4.45	52.58	N/A	N/A	8.8	N/A	5.77	N/A	4.41	0.222
14	1	G-M	3.87	60.47	15.56	11.46	N/A	8.53	N/A	2.87	N/A	N/A
15	2	M-G	4.76	49.16	N/A	N/A	7.01	N/A	4.14	N/A	1.86	0.11
16	1	G-M	3.18	73.58	17.67	11.05	N/A	8.5	N/A	4.42	N/A	N/A

17	1	G-M	3.44	68.02	16.5	12.94	N/A	7.25	N/A	3.02	N/A	N/A
18	2	M-G	3.48	67.24	28.54	22.38	N/A	16.36	N/A	12.01	N/A	N/A
19	1	G-M	3.14	74.52			N/A		N/A		N/A	N/A
20	1	G-M	3.02	77.48	17.37	11.95	N/A	7.06	N/A	3.2	N/A	N/A
21	1	G-M	4.57	51.20	12.22	8.91	N/A	5.41	N/A	2.54	N/A	N/A
22	1	G-M	3.67	63.76	16.098	10.84	N/A	6.51	N/A	2.523	N/A	N/A
23	2	G-M	6.01	38.94	N/A	N/A	5.13	N/A	1.63	N/A	N/A	N/A
24	1	G-M	4.12	56.80	15.26	11.25	N/A	7.216	N/A	3.27	N/A	N/A
25	1	G-M	3.01	77.74	17.588	13.13	N/A	8.073	N/A	3.24	N/A	N/A

26	2	M-G	5.74	40.77	N/A	N/A	5.315	N/A	3.379	N/A	N/A	0.969
27	1	M-G	5.49	42.62	9.89	6.18	N/A	2.89	N/A	0.797	N/A	N/A

Appendix D: The schematic diagram of a) STEVAL-MKI180V1 sensor and b) Raspberry Pi

a)

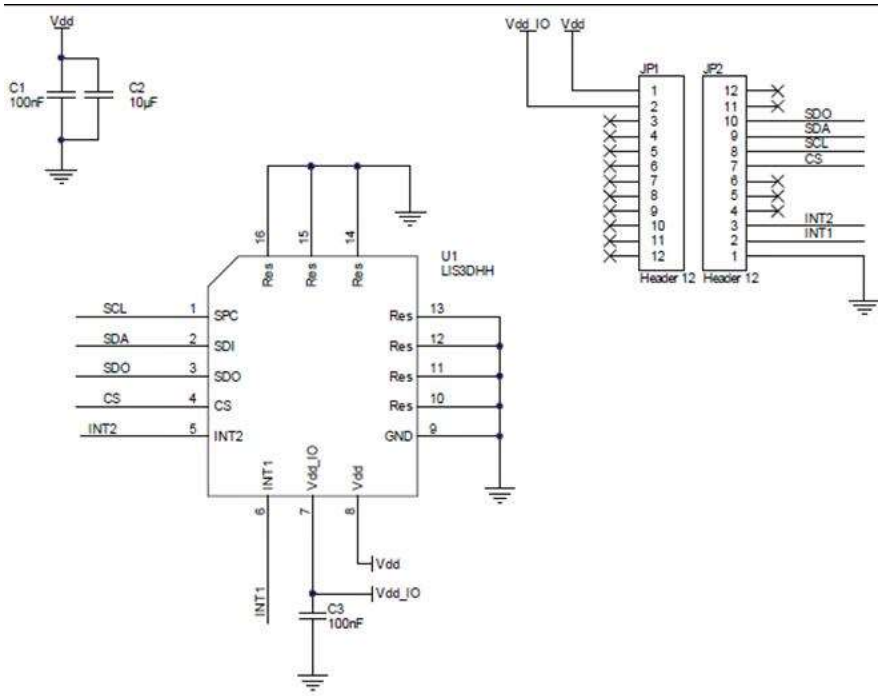

b)